

Refining neural network predictions using background knowledge

Alessandro Daniele^{1†}, Emile van Krieken^{2†}, Luciano Serafini¹
and Frank van Harmelen²

¹Data and Knowledge Management unit, Fondazione Bruno Kessler, via Sommarive 18, Trento, 38123, Italy.

²Department of Computer Science, Vrije Universiteit Amsterdam, de Boelelaan 1081a, Amsterdam, 1081HV, Netherlands.

Contributing authors: daniele@fbk.eu; e.van.krieken@vu.nl;

[†]These authors contributed equally to this work.

Abstract

Recent work has shown logical background knowledge can be used in learning systems to compensate for a lack of labeled training data. Many methods work by creating a loss function that encodes this knowledge. However, often the logic is discarded after training, even if it is still useful at test time. Instead, we ensure neural network predictions satisfy the knowledge by refining the predictions with an extra computation step. We introduce differentiable *refinement functions* that find a corrected prediction close to the original prediction. We study how to effectively and efficiently compute these refinement functions. Using a new algorithm called Iterative Local Refinement (ILR), we combine refinement functions to find refined predictions for logical formulas of any complexity. ILR finds refinements on complex SAT formulas in significantly fewer iterations and frequently finds solutions where gradient descent can not. Finally, ILR produces competitive results in the MNIST addition task.

1 Introduction

Recent years have shown promising examples of using symbolic background knowledge in learning systems: From training classifiers with weak supervision signals [25], generalizing learned classifiers to new tasks [29], compensating for

a lack of good supervised data [9, 10], to enforcing the structure of outputs through a logical specification [34]. The main idea underlying these integrations of learning and reasoning, often called neuro-symbolic integration, is that background knowledge can complement the neural network when one lacks high-quality labeled data [16]. Although pure deep learning approaches excel when learning over *vast* quantities of data with *gigantic* amounts of compute [5, 27], most tasks are not afforded this luxury.

Many neuro-symbolic methods work by creating a differentiable loss function that encodes the background knowledge (Figure 1a). However, often the logic is discarded after training, even though this background knowledge could still be helpful at test time [15, 29]. Instead, we ensure we constrain the neural network with the background knowledge, both during train time and test time, by correcting its output such that it will satisfy the background knowledge (Figure 1b). In particular, we consider how to make such corrections while being as close as possible to the original predictions of the neural network.

We study how to effectively and efficiently correct the neural network by ensuring its predictions satisfy the symbolic background knowledge. In particular, we consider fuzzy logics formed using functions called t-norms [23, 28]. Prior work has shown how to use a gradient ascent-based optimization procedure to find a prediction that satisfies this fuzzy background knowledge [9, 29]. However, a recent model called KENN [7] shows how to compute the correction analytically for a fragment of the Gödel logic.

To extend this line of work, we introduce the concept of *refinement functions*, and derive refinement functions for many fuzzy logic operators. Refinement functions are functions that find a prediction that satisfies the background knowledge while staying close to the neural network’s original prediction. Using a new algorithm called *Iterative Local Refinement* (ILR), we can combine refinement functions for different fuzzy logic operators to efficiently find refinements for logical formulas of any complexity. Since refinement functions are differentiable, we can easily integrate them as a neural network layer. In our experiments, we compare ILR with an approach using gradient ascent. We find that ILR finds optimal refinements in significantly fewer iterations. Moreover, ILR often produces results that stay closer to the original predictions or better satisfy the background knowledge. Finally, we evaluated ILR on the MNIST Addition task [25] and show that ILR can be combined with neural networks to solve common neuro-symbolic tasks.

In summary, our contributions are:

1. We formalize the concept of minimal refinement functions in Section 4.
2. We introduce the ILR algorithm in Section 5, which uses the minimal refinement functions for individual fuzzy operators to find refinements for general logical formulas.
3. We discuss how to use ILR for neuro-symbolic AI in Section 6, where we exploit the fact that ILR is a differentiable algorithm.

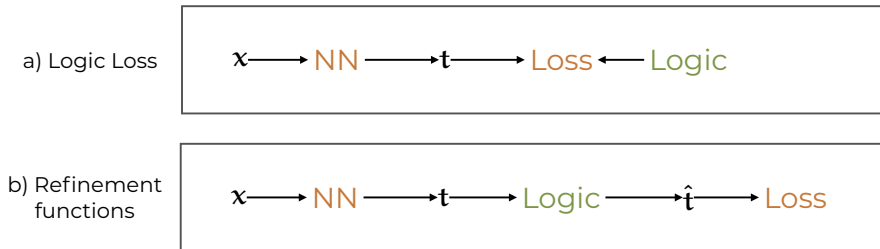


Fig. 1 Comparing different approaches for constraining neural networks with background knowledge. Loss-based approaches include LTN, SBR, and Semantic Loss, while KENN, C-HMCNN(h), and SBR-CC are representatives for refinement functions.

4. We analytically derive minimal refinement functions for individual fuzzy operators constructed from the Gödel, Łukasiewicz, and product t-norms in Section 7.2.
5. We discuss a large class of t-norms for which we can analytically derive minimal refinement functions in Section 7.
6. We compare ILR to gradient descent approaches and show it finds refinements on complex SAT formulas in significantly fewer iterations and frequently finds solutions where gradient descent can not.
7. We apply ILR to the MNIST Addition task [25] to test how ILR behaves when injecting knowledge into neural network models.

2 Related work

ILR falls into a larger body of work that attempts to integrate background knowledge expressed as logical formulas into neural networks. For an overview, see [16]. As shown in Figure 1, methods can be categorized by whether they only use background knowledge during training in the form of a loss function [3, 9, 12, 32, 34, 35] or whether the background knowledge is part of the model and therefore enforces the knowledge also at test time [1, 7, 11, 14, 17, 33]. ILR is a method in the second category. We note that these approaches can be combined [15, 29].

First, we discuss approaches that construct loss functions from the logical formulas (Figure 1a). These loss functions measure when the deep learning model violates the background knowledge, such that minimizing the loss function amounts to “correcting” such violations [32]. While these methods show significant empirical improvement, they do not guarantee that the neural network will satisfy the formulas outside the training data. LTN and SBR [3, 9] use fuzzy logic to provide compatibility with neural network learning, while Semantic Loss [34] uses probabilistic logics. The formalization of refinement functions can be extended to probabilistic logics by defining a suitable notion of minimality, like the KL-divergence between the original and refined distributions over ground atoms.

Name	T-norm
Minimum	$T_G(\mathbf{t}) = \min_{i=1}^n t_i$
Product	$T_P(\mathbf{t}) = \prod_{i=1}^n t_i$
Lukasiewicz	$T_L(\mathbf{t}) = \max(\sum_{i=1}^n t_i - (n-1), 0)$

Table 1 Some common t-norms extended to any-arity aggregation operators.

Among the methods where knowledge is part of the model, KENN inspired ILR [7, 8]. KENN is a framework that injects knowledge into neural networks by iteratively refining its predictions. It uses a relaxed version of the Gödel t-conorm obtained through a relaxation of the argmax function, which it applies in logit space. Closely related to both ILR and KENN is C-HMCNN(h) [14], which we see as computing the minimal refinement function for stratified normal logic programs under Gödel t-norm semantics. We discuss this connection in more detail in Section 7.2.1.

The loss-function based method SBR also introduces a procedure for using the logical formulas at test time in the context of collective classification [9, 29]. Unlike KENN [7], these approaches do not enforce the background knowledge during training but only use it as a test time procedure. In particular, [29] shows that doing these corrections at test time improves upon just using the loss-function approach. Unlike our analytic approach to refinement functions, SBR finds new predictions using a gradient descent procedure very similar to the algorithm we discuss in Section 9.1.2. We show it is much slower to compute than ILR.

Another method closely related to ILR is the neural network layer SATNet [33], which has a setup closely related to ours. However, SATNet does not have a notion like minimality and uses a different underlying logic constructed from a semidefinite relaxation. DeepProbLog [25] also is a probabilistic logic, but unlike Semantic Loss is used to derive new statements through proofs and cannot directly be used to correct the neural network on predictions that do not satisfy the background knowledge. Instead, ILR can be used both for injecting constraints on the output of a neural network, as well as for proving new statements starting from the neural network predictions.

Finally, some methods are limited to equality and inequality constraints rather than general symbolic background knowledge [12, 17]. DL2 [12] combines these constraints into a real-valued loss function, while MultiplexNet [17] adds the knowledge as part of the model. However, MultiplexNet requires expressing the logical formulas as a DNF formula, which is hard to scale.

3 Fuzzy Operators

We will first provide the necessary background knowledge for defining and analyzing minimal refinement functions. In particular, we will consider fuzzy operators, which generalize the connectives of classical boolean logic. For formal treatments of the study of such operators, we refer the reader to [23], which discusses t-norms and t-conorms, to [20] for fuzzy implications, to [4] for aggregation functions, and to [32] for an analysis of the derivatives of these operators.

Definition 1. A function $T : [0, 1]^2 \rightarrow [0, 1]$ is a *t-norm* (triangular norm) if it is commutative, associative, increasing in both arguments, and if for all $t \in [0, 1]$, $T(1, t) = t$.

Similarly, a function $S : [0, 1]^2 \rightarrow [0, 1]$ is a *t-conorm* if the last condition instead is that for all $t \in [0, 1]$, $S(0, t) = t$.

Dual t-conorms are formed from a t-norm T using $S(t_1, t_2) = 1 - T(1 - t_1, 1 - t_2)$. We list any-arity extensions, constructed using $T(\mathbf{t}) = T(t_1, T(t_{2:n}))$, $T(t_i) = t_i$ of five basic t-norms in Table 1. Here $\mathbf{t} = [t_1, \dots, t_n]^\top \in [0, 1]^n$ is a vector of fuzzy truth values, which we will often refer to as (*truth*) *vectors*. These any-arity extensions are examples of fuzzy aggregation operators [4].

Definition 2. A t-norm T is *Archimedean* if for all $x, y \in (0, 1)$, there is an n such that $T(\underbrace{x, \dots, x}_{n \times}) < y$.

A continuous t-norm T is *strict* if, in addition, for all $x \in (0, 1)$, $0 < T(x, x) < x$.

Definition 3. A function $I : [0, 1]^2 \rightarrow [0, 1]$ is a *fuzzy implication* if for all $t_1, t_2 \in [0, 1]$, $I(\cdot, t_2)$ is decreasing, $I(t_1, \cdot)$ is increasing and if $I(0, 0) = 1$, $I(1, 1) = 1$ and $I(1, 0) = 0$.

Note that fuzzy implications do not have n -ary extensions as they are not associative. The so-called *S-implications* are formed from the t-conorm by generalizing the material implication using $I(a, c) = S(1 - a, c)$. Furthermore, every t-norm induces a unique *residuum* or *R-implication* [20] $R_T(a, c) = \sup\{z | T(z, a) \leq c\}$.

Logical formulas φ can be evaluated using compositions of fuzzy operators. We assume φ is a propositional logic formula, but note this evaluation procedure can be extended to grounded first-order logical formulas on finite domains. For instance, [8] introduced a technique for propositionalizing universally quantified formulas of predicate logic in the context of KENN. Moreover, this technique can be extended to existential quantification by treating it as a disjunction. We assume a set of propositions $\mathcal{P} = \{P_1, \dots, P_n\}$ and constants $\mathcal{C} = \{C_1, \dots, C_m\}$, where each constant has a fixed value $C_i \in [0, 1]$.

Definition 4. If T is a t-norm, S a t-conorm and I a fuzzy implication, then the *fuzzy evaluation operator* $f_\varphi : [0, 1]^n \rightarrow [0, 1]$ of the formula φ with propositions \mathcal{P} and constants \mathcal{C} is a function of truth vectors \mathbf{t} and given as

$$f_{P_i}(\mathbf{t}) = t_i \tag{1}$$

$$f_{C_j}(\mathbf{t}) = C_j \tag{2}$$

$$f_{\neg\phi}(\mathbf{t}) = 1 - f_\phi(\mathbf{t}) \tag{3}$$

$$f_{\bigwedge_{j=1}^m \phi_j}(\mathbf{t}) = T(f_{\phi_1}(\mathbf{t}), \dots, f_{\phi_m}(\mathbf{t})) \tag{4}$$

$$f_{\bigvee_{j=1}^m \phi_j}(\mathbf{t}) = S(f_{\phi_1}(\mathbf{t}), \dots, f_{\phi_m}(\mathbf{t})) \quad (5)$$

$$f_{\phi \rightarrow \psi}(\mathbf{t}) = I(f_{\phi}(\mathbf{t}), f_{\psi}(\mathbf{t})). \quad (6)$$

where we match on the structure of the formula φ in the subscript f_{φ} .

4 Minimal Fuzzy Refinement Functions

We will next define (fuzzy) refinement functions, which consider how to change the input arguments of fuzzy operators such that the output of the operators is a given truth value. We prefer changes to the input arguments that are as small as possible. We will introduce several definitions to facilitate studying this concept. The first is an optimality criterion.

Definition 5 (Fuzzy refinement function). Let $f_{\varphi} : [0, 1]^n \rightarrow [0, 1]$ be a fuzzy evaluation operator. Then $\hat{\mathbf{t}} : [0, 1]^n$ is called a *refined (truth) vector* for the *refinement value* $\hat{t}_{\varphi} \in [0, 1]$ if $f_{\varphi}(\hat{\mathbf{t}}) = \hat{t}_{\varphi}$.

Furthermore, let $\min_{\varphi} = \min_{\hat{\mathbf{t}} \in [0, 1]^n} f_{\varphi}(\hat{\mathbf{t}})$ and $\max_{\varphi} = \max_{\hat{\mathbf{t}} \in [0, 1]^n} f_{\varphi}(\hat{\mathbf{t}})$. Then $\rho : [0, 1]^n \times [0, 1] \rightarrow [0, 1]^n$ is a (*fuzzy*) *refinement function*¹ for f_{φ} if for all $\mathbf{t} \in [0, 1]^n$,

1. for all $\hat{t}_{\varphi} \in [\min_{\varphi}, \max_{\varphi}]$, $\rho(\mathbf{t}, \hat{t}_{\varphi})$ is a refined vector for \hat{t}_{φ} ;
2. for all $\hat{t}_{\varphi} < \min_{\varphi}$, $\rho(\mathbf{t}, \hat{t}_{\varphi}) = \rho(\mathbf{t}, \min_{\varphi})$;
3. for all $\hat{t}_{\varphi} > \max_{\varphi}$, $\rho(\mathbf{t}, \hat{t}_{\varphi}) = \rho(\mathbf{t}, \max_{\varphi})$.

A refinement function for f_{φ} changes the input truth vector in such a way that the new output of f_{φ} will be \hat{t}_{φ} . Whenever \hat{t}_{φ} is high, we want the refined vector to satisfy the formula φ , while if \hat{t}_{φ} is low, we want it to satisfy its negation. When $\hat{t}_{\varphi} = 1$, the constraint created by the formula is a hard constraint, while if it is in $(0, 1)$, this constraint is soft. We require bounding the set of possible \hat{t}_{φ} by \min_{φ} and \max_{φ} , since if there are constants C_i , or if φ has no satisfying (discrete) solutions, there can be formulas such that there can be no refined vectors $\hat{\mathbf{t}}$ for which $f_{\varphi}(\hat{\mathbf{t}})$ equals 1.

Next, we introduce a notion of minimality of refinement functions. The intuition behind this concept is that we prefer the new output, the refined vector $\hat{\mathbf{t}}$, to stay as close as possible to the original truth vector \mathbf{t} . Therefore, we assume we want to find a truth vector near the neural network's output that satisfies the background knowledge.

Definition 6 (Minimal refinement function). Let ρ^* be a refinement function for operator f_{φ} . ρ^* is a *minimal* refinement function with respect to some norm $\|\cdot\|$ if for each $\mathbf{t} \in [0, 1]^n$ and $\hat{t}_{\varphi} \in [\min_{\varphi}, \max_{\varphi}]$, there is no refined vector $\hat{\mathbf{t}}'$ for \hat{t}_{φ} such that $\|\rho^*(\mathbf{t}, \hat{t}_{\varphi}) - \mathbf{t}\| > \|\hat{\mathbf{t}}' - \mathbf{t}\|$.

¹The concept of refinement functions is closely related to the concept of *Fuzzy boost function* in the KENN paper [7].

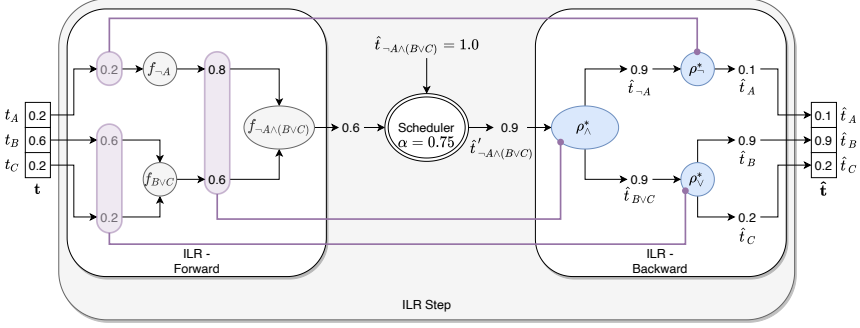


Fig. 2 Visualization of one step of ILR for the Gödel logic and formula $\phi = \neg A \wedge (B \vee C)$. In the forward pass (left), ILR computes the truth value of ϕ . In the backward pass (right), ILR traverses the computational graph of the forward step in reverse to calculate the refined vector $\hat{\mathbf{t}}$. ILR substitutes each fuzzy operator of the forward pass with the corresponding refinement function. Each refinement function receives as input the initial truth values used by the fuzzy operator in the forward step (purple lines) and the target value for the corresponding subformula. The scheduler calculates the target value $i'_{\neg A \wedge (B \vee C)}$ for the entire formula, which ILR calls between the forward and backward steps.

For a particular fuzzy evaluation operator f_φ , finding the minimal refinement function corresponds to solving the following optimization problem:

$$\begin{aligned}
 &\text{For all } \mathbf{t} \in [0, 1]^n, \hat{\mathbf{t}}_\varphi \in [\min_\varphi, \max_\varphi] \\
 &\quad \min_{\hat{\mathbf{t}}} \|\hat{\mathbf{t}} - \mathbf{t}\| \\
 &\quad \text{such that } f_\varphi(\hat{\mathbf{t}}) = \hat{\mathbf{t}}_\varphi, \\
 &\quad \quad \quad 0 \leq \hat{t}_i \leq 1
 \end{aligned} \tag{7}$$

For some f_φ we can solve this problem analytically using the Karush-Kuhn-Tucker (KKT) conditions. However, while $\|\cdot\|$ is convex, f_φ (usually) is not. Therefore, we can not rely on efficient convex solvers. Furthermore, for strict t-norms, finding exact solutions to this problem is equivalent to solving PMaxSAT when $\hat{t}_\varphi = 1$ [9, 15], hence this problem is NP-complete. In Sections 7 and 8, we will analytically derive minimal refinement functions for a large amount of individual fuzzy operators. These results are the theoretical contribution of this paper. We first discuss in Section 5 a method called ILR for finding general solutions to the problem of finding minimal refinement functions. ILR uses the analytical minimal refinement functions of individual fuzzy operators in a forward-backward algorithm. Then, in Section 6, we discuss how to use this algorithm for neuro-symbolic AI.

5 Iterative Local Refinement

We introduce a fast, iterative, differentiable but approximate algorithm called *Iterative Local Refinement (ILR)* that finds minimal refinement functions for general formulas. ILR is a forward-backward algorithm acting on the computation graph of formulas. First, it traverses the graph from its leaves to its

root to compute the current truth values of subformulas. Then, it traverses the graph back from its root to the leaves to compute new truth values for the subformulas. ILR makes use of analytical minimal refinement functions to perform this backward pass. ILR is a differentiable algorithm if the fuzzy operators and their corresponding minimal refinement functions are differentiable as it computes compositions of these functions. An example of one step of the ILR algorithm is presented in Figure 2, while Algorithm 1 contains the entire pseudocode.

First, ILR computes the truth value of the formula in the forward pass (left side of Figure 2), where the truth vectors of intermediate subformulas are saved (in Algorithm 1: \mathbf{t}_{sub} . In Figure 2: numbers inside colored boxes). Then, ILR computes a backward pass (right side of Figure 2). ILR uses previously computed truth vectors of subformulas to compute the minimal refined vectors for the components of that subformula. We use the results from Sections 7.2 to compute these for the Gödel, Lukasiewicz and product fuzzy operators.

In lines 13 to 19, ILR computes the minimal refined vector for a conjunction of subformulas. We retrieve the truth values of the subformulas from the forward pass and call the minimal refinement function ρ_T^* for the chosen t-norm. This procedure gives us a refined vector, where each value corresponds to the refined value of a subformula. ILR then goes in recursion on the subformulas. Note that the pseudocode for disjunction and implication is analogous.

One choice in ILR is how to combine the results from different subformulas. When a proposition appears in multiple subformulas, it can be assigned multiple different refined values. We found the heuristic in line 18 generally works well, which takes the \hat{t}_j with the largest absolute value. We also explored averaging the different refined values, but this took significantly longer to converge. Another choice is the convergence criterion. A simple option is to stop running the algorithm whenever it has stopped getting closer to the refined value for a couple of iterations. In our experiments, we observed that ILR monotonically decreases the distance to the refined value, after which it gets stuck either on a single local optimum or oscillates between two local minima.

Moreover, we experimented with a scheduling mechanism to smooth the behavior of ILR. We implement this in line 6. The scheduling mechanism works by choosing a different refined value at each iteration: The difference between the current truth value and the refined value is multiplied by a scheduling parameter α , which we choose to be either 0.1 or 1 (no scheduling). While usually not necessary, for some formulas, the scheduling mechanism allowed for finding better solutions.

ILR is not guaranteed to find a refined vector $\hat{\mathbf{t}}$ such that $f_\varphi(\hat{\mathbf{t}}) = \hat{t}_\varphi$. This is easy to see theoretically because, for many fuzzy logics like the product and Gödel logics, $\hat{t}_\varphi = 1$ corresponds to the PMaxSAT problem, which is NP-complete [9, 15], while ILR has linear time complexity. However, this is traded off by 1) being highly efficient, usually requiring only a couple of iterations for convergence, and 2) not having any hyperparameters to tune, except arguably for the combination function. Furthermore, ILR usually converges

quickly in neuro-symbolic settings since background knowledge is very structured, and the solution space is relatively dense. These settings are unlike the randomly generated SAT problems we study in Section 9.1.3. These contain little structure the ILR algorithm can exploit.

Algorithm 1 Iterative Local Refinement

Require: $\varphi, \hat{t}_\varphi, \mathbf{t}, \alpha \in (0, 1]$

- 1: $\mathbf{t}' \leftarrow \mathbf{t}$
- 2: **while** not converged **do**
- 3: $\mathbf{t}_{\text{sub}} \leftarrow \{\}$
- 4: **for** subformula ϕ of φ **do**
- 5: $\mathbf{t}_{\text{sub}}[\phi] \leftarrow f_\phi(\mathbf{t}')$ ▷ Forward pass using Definition 4
- 6: $\hat{t}'_\varphi \leftarrow f_\varphi(\mathbf{t}) + (\hat{t}_\varphi - f_\varphi(\mathbf{t}))\alpha$
- 7: $\mathbf{t}' \leftarrow \text{BACKWARD}(\varphi, \hat{t}'_\varphi, \mathbf{t}_{\text{sub}})$
- 8: **return** \mathbf{t}'
- 9: **function** BACKWARD($P_i, \hat{t}_{P_i}, \mathbf{t}_{\text{sub}}$)
- 10: **return** $[t_1, \dots, \hat{t}_{P_i}, \dots, t_n]^\top$ ▷ \mathbf{t} except at position i .
- 11: **function** BACKWARD($\neg\phi, \hat{t}_{\neg\phi}, \mathbf{t}_{\text{sub}}$)
- 12: **return** BACKWARD($\phi, 1 - \hat{t}_{\neg\phi}, \mathbf{t}_{\text{sub}}$)
- 13: **function** BACKWARD($\bigwedge_{i=1}^m \phi_i, \hat{t}_\varphi, \mathbf{t}_{\text{sub}}$)
- 14: $\hat{\mathbf{t}}_\wedge \leftarrow \rho_T^*([\mathbf{t}_{\text{sub}}[\phi_1], \dots, \mathbf{t}_{\text{sub}}[\phi_m]]^\top, \hat{t}_\varphi)$ ▷ Minimal refinement function
- 15: $\hat{\mathbf{t}} \leftarrow \mathbf{0}$
- 16: **for** $i \leftarrow 1$ to m **do**
- 17: $\hat{\mathbf{t}}' \leftarrow \text{BACKWARD}(\phi_i, \hat{t}_{\wedge, i}, \mathbf{t}_{\text{sub}})$
- 18: $\hat{t}_j \leftarrow \text{if } |\hat{t}_j| > |\hat{t}'_j| \text{ then } \hat{t}_j \text{ else } \hat{t}'_j \text{ for all } j \in \{1, \dots, n\}$
- 19: **return** $\hat{\mathbf{t}}$

6 Neuro-Symbolic AI using ILR

The ILR algorithm can be added as a module after a neural network g to create a neuro-symbolic AI model. The neural network predicts (possibly some of) the initial truth values \mathbf{t} . Since both the forward and backward passes of ILR are differentiable computations, we can treat ILR as a constrained output layer [16]. For instance, in Figure 2, the input \mathbf{t} could be generated by the neural network, and we provide supervision directly on the predictions $\hat{\mathbf{t}}$. ILR ensures the predictions, i.e., the refined vector $\hat{\mathbf{t}}$, satisfy the background knowledge while staying close to the original predictions made by the neural network. Loss functions like cross-entropy can use $\hat{\mathbf{t}}$ as the prediction. We train the neural network g by minimizing the loss function with gradient descent and backpropagating through the ILR layer.

One strength of ILR is the flexibility of the refinement values \hat{t}_{φ_i} for each formula φ_i . These can be set to 1 to treat φ_i as a hard constraint that always needs to be satisfied. Alternatively, refinement values can be trained as part of a larger deep learning model. Since ILR is a differentiable layer, we can compute gradients of the refinement values. This procedure allows ILR to learn what formulas are useful for prediction. For instance, in Figure 2, $\hat{t}_{\neg A \wedge (B \vee C)}$ can either be given or act as a parameter of the model that is learned together with the neural network parameters.

We give an example of the integration of ILR with a neural network in Figure 3, where we use ILR for the MNIST Addition task proposed by [25]. In this task, we have access to a training set composed of triplets (x, y, z) , where x and y are images of MNIST [24] handwritten digits, and z is a label representing an integer in the range $\{0, \dots, 18\}$, corresponding to the sum of the digits represented by x and y . The task consists of learning the addition function and a classifier for the MNIST digits, with supervision only on the sums. To achieve this, knowledge consisting of the rules of addition is given. For instance, the rule $Is(x, 3) \wedge Is(y, 2) \rightarrow Is(x + y, 5)$ states that the sum of 3 and 2 is 5.

The architecture of Figure 3 consists of a neural network (a CNN) that performs digit recognition on the inputs x and y . After this step, ILR predicts a truth value for each possible sum. Notice that we define the CNN outputs $\mathbf{C}_x, \mathbf{C}_y \in [0, 1]^{10}$ as constants, i.e., ILR does not change the predictions of the digits. Moreover, the initial prediction for the truth vector of possible sums $\hat{\mathbf{t}}_{x+y} \in [0, 1]^{19}$ is the zero vector. This allows ILR to act as a proof-based method. Indeed, similarly to DeepProbLog [25], the architecture proposed in Figure 3 uses the knowledge in combination with the predictions of the neural network to derive truth values for new statements (the sum of the two digits). We apply the loss function to the final predictions $\hat{\mathbf{t}}_{x+y}$. During learning, the error is back-propagated through the entire model, reaching the CNN, which learns to classify the MNIST images from indirect supervision.

We present the results obtained by ILR in Section 9.2, and compare its performance with other neuro-symbolic AI frameworks.

7 Analytical minimal refinement functions

Having introduced the ILR algorithm, we next study the problem of finding minimal refinement functions for individual fuzzy operators. We need these in closed form to compute the ILR algorithm, as ILR uses them during the backward pass. This section first discusses several transformations of minimal refinement functions and gives the minimal refinement functions of the basic t-norms Gödel, Lukasiewicz and product. In Section 7 we investigate a large class of t-norms for which we have closed-form formulas for the minimal refinement functions.

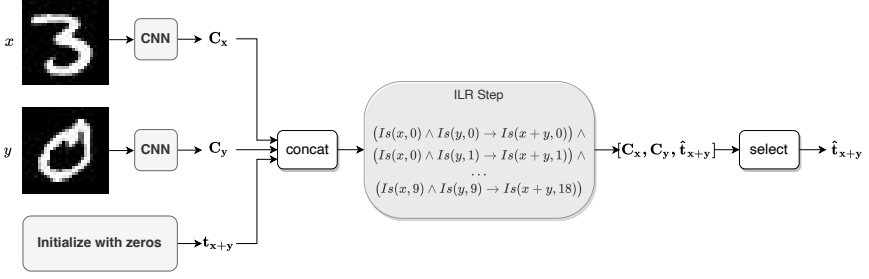


Fig. 3 Neuro-symbolic architecture based on ILR for the MNIST Addition task. A CNN takes in input two images of MNIST digits, returning their classification. The predictions of the CNN are concatenated together with a vector of zeros, representing the initial prediction for the Addition task. We perform an ILR step to update the sum of the two numbers, which is the final output of the model.

7.1 General results

We first provide several basic results on minimal refinement functions for fuzzy operators. In particular, we will consider formulas such as $\varphi = \bigwedge_{i=1}^n P_i \bigwedge_{i=1}^m C_i$, that is, conjunctions of propositions and constants. As abuse of notation, from here on, we will refer to \min_φ and \max_φ when evaluated by the t-norm T as \min_T and \max_T and will do so also for other fuzzy operators. We find using Definition 1 that for some t-norm T , $\min_T = 0$ and $\max_T = T(\mathbf{c})$, where \mathbf{c} is the values of the constants C_1, \dots, C_m as a truth vector, while for some t-conorm S , $\min_S = S(\mathbf{c})$ and $\max_S = 1$. Note that for $m = 0$, $\max_T = 1$ and $\min_S = 0$. Next, we find some useful transformations of minimal refinement functions to derive new results:

Proposition 1. Consider the formulas $\phi = \bigwedge_{i=1}^n P_i \bigwedge_{i=1}^m C_i$ and $\psi = \neg(\bigvee_{i=1}^n P_i \bigvee_{i=1}^m C_i)$. Assume ρ_ϕ^* is a minimal refinement function for f_ϕ evaluated using t-norm T . Consider $f_\psi(\mathbf{t})$ evaluated using dual t-conorm S of T . Then $\rho_\psi^*(\mathbf{t}, \hat{\mathbf{t}}_\psi) = \mathbf{1} - \rho_\phi^*(\mathbf{1} - \mathbf{t}, \hat{\mathbf{t}}_\psi)$ is a minimal refinement function for f_ψ .

Proof First, note $f_\psi(\mathbf{t}) = 1 - S(\mathbf{t}, \mathbf{c}) = 1 - (1 - T(\mathbf{1} - \mathbf{t}, \mathbf{1} - \mathbf{c})) = T(\mathbf{1} - \mathbf{t}, \mathbf{1} - \mathbf{c})$. Consider $\mathbf{t}' = \mathbf{1} - \mathbf{t}$. By the assumption of the proposition, $\rho_\phi^*(\mathbf{t}', \hat{\mathbf{t}}_\phi)$ is a minimal refinement function for $T(\mathbf{t}', \mathbf{1} - \mathbf{c}) = T(\mathbf{1} - \mathbf{t}, \mathbf{1} - \mathbf{c}) = f_\psi(\mathbf{t})$. Furthermore, note that

$$f_\psi(\rho_\psi^*(\mathbf{t}, \hat{\mathbf{t}}_\psi)) = T(\mathbf{1} - \rho_\psi^*(\mathbf{t}, \hat{\mathbf{t}}_\psi), \mathbf{1} - \mathbf{c}) = T(\rho_\phi^*(\mathbf{t}', \hat{\mathbf{t}}_\psi), \mathbf{1} - \mathbf{c}) = \hat{\mathbf{t}}_\psi$$

□

An analogous argument can be made for $\phi' = \bigvee_{i=1}^n P_i \bigvee_{i=1}^m C_i$ and $\psi = \neg(\bigwedge_{i=1}^n P_i \bigwedge_{i=1}^m C_i)$ to show that, given minimal refinement function $\rho_{\phi'}^*$ of dual t-conorm S , the minimal refinement function for $f_\psi(\mathbf{t})$ is $\rho_\psi^*(\mathbf{t}, \hat{\mathbf{t}}_\psi) = \mathbf{1} - \rho_{\phi'}^*(\mathbf{1} - \mathbf{t}, \hat{\mathbf{t}}_\psi)$.

We will use this result to simplify the process of finding minimal refinement functions for the t-norms and dual t-conorms. For example, assume we have a minimal refinement function ρ_T^* for $\hat{\mathbf{t}}_T \in [T(\mathbf{t}), \max_T]$. Let S be the

corresponding dual t-conorm. Then, we can change the constraint $S(\hat{\mathbf{t}}, \mathbf{c}) = \hat{t}_S$ in Equation 7 to the equivalent constraint $\mathbf{1} - S(\hat{\mathbf{t}}, \mathbf{c}) = \mathbf{1} - \hat{t}_S$. We then use Proposition 1 to find the minimal refined vector for $\hat{t}_S \in [\min_S, S(\mathbf{t})]$ as $\mathbf{1} - \rho_T^*(\mathbf{1} - \mathbf{t}, \mathbf{1} - \hat{t}_S)$.

Proposition 2. *Consider the formulas $\phi = P_1 \vee P_2$ and $\psi = \neg P_1 \vee P_2$. Assume ρ_ϕ^* is a minimal refinement function for f_ϕ evaluated using the t-conorm S , and define $\mathbf{t}' = [1 - t_1, t_2]$. Then $\rho_\psi^*(\mathbf{t}, \hat{t}_\psi) = \left[1 - \rho_\phi^*(\mathbf{t}', \hat{t}_\psi)_1, \rho_\phi^*(\mathbf{t}', \hat{t}_\psi)_2\right]^\top$ is a minimal refinement function for f_ψ .*

Proof First, note $f_\psi(\mathbf{t}) = S(1 - t_1, t_2)$. By the assumption of the proposition, $\rho_\phi^*(\mathbf{t}', \hat{t}_\psi)$ is a minimal refinement function for $S(\mathbf{t}') = f_\psi(\mathbf{t})$. Furthermore, note that

$$\begin{aligned} f_\psi(\rho_\psi^*(\mathbf{t}, \hat{t}_\psi)) &= S(1 - \rho_\psi^*(\mathbf{t}, \hat{t}_\psi)_1, \rho_\psi^*(\mathbf{t}, \hat{t}_\psi)_2) \\ &= S(1 - (1 - \rho_\phi^*(\mathbf{t}', \hat{t}_\psi)_1), \rho_\phi^*(\mathbf{t}', \hat{t}_\psi)_2) = S(\rho_\phi^*(\mathbf{t}', \hat{t}_\psi)) = \hat{t}_\psi. \end{aligned}$$

□

Similar to the previous proposition, this proposition gives us a simple procedure for finding the minimal refinement functions for the S-implication of some t-conorm.

7.2 Basic T-norms

In this section, we introduce the minimal refinement functions for the t-norms and t-conorms of the three main fuzzy logics (Gödel, Lukasiewicz, and Product). In particular, we consider when these t-norms and t-conorms can act on both propositions and constants, that is, $\varphi = \bigwedge_{i=1}^n t_i \bigwedge_{i=1}^m C_i$, which is evaluated with $T(\mathbf{t}, \mathbf{c})$. We present the main results with simple examples.

7.2.1 Gödel t-norm

In this section, we derive minimal refinement functions for the Gödel t-norm and t-conorm for the family of p -norms.

Proposition 3. *The minimal refinement function of the Gödel t-norm for $\hat{t}_{T_G} \in [0, \min_{i=1}^m C_i]$ is*

$$\rho_{T_G}^*(\mathbf{t}, \hat{t}_{T_G})_i = \begin{cases} \hat{t}_{T_G} & \text{if } \hat{t}_{T_G} \geq T_G(\mathbf{t}) \text{ and } t_i < \hat{t}_{T_G}, \\ \hat{t}_{T_G} & \text{if } \hat{t}_{T_G} < T_G(\mathbf{t}) \text{ and } i = \arg \min_{j=1}^n t_j, \\ t_i & \text{otherwise,} \end{cases} \quad (8)$$

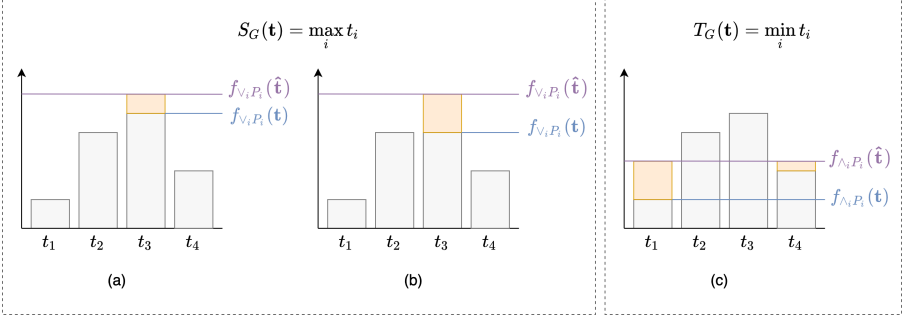


Fig. 4 Gödel minimal refinement functions. The grey bars represent the initial truth vectors \mathbf{t} ; the light blue and purple lines indicate the initial truth value of the formula and the revision value \hat{t}_φ , and the orange bars are the corresponding minimal refined vectors. (a) t-conorm; (b) t-conorm with two literals with same truth value; (c) t-norm.

The minimal refinement function of the Gödel t-conorm and $\hat{t}_{S_G} \in [\max_{i=1}^m C_i, 1]$ is

$$\rho_{S_G}^*(\mathbf{t}, \hat{t}_{S_G})_i = \begin{cases} \hat{t}_{S_G} & \text{if } \hat{t}_{S_G} \geq S_G(\mathbf{t}) \text{ and } i = \arg \max_{j=1}^m t_j, \\ \hat{t}_{S_G} & \text{if } \hat{t}_{S_G} < S_G(\mathbf{t}) \text{ and } t_i > \hat{t}_{S_G}, \\ 0 & \text{otherwise.} \end{cases} \quad (9)$$

Proof Follows from Propositions 1, 10 and 11, see Appendix A.1.1 and A.1.2. \square

Proposition 4. A minimal refinement function of the Gödel implication

$$R_G(t_1, t_2) = \begin{cases} t_2 & \text{if } t_1 > t_2, \\ 1 & \text{otherwise.} \end{cases} \text{ for } \hat{t}_{R_G} \in [\min_{R_G}, \max_{R_G}] \text{ is}$$

$$\rho_{R_G}^*(t_1, t_2, \hat{t}_{R_G}) = \begin{cases} [\max(\hat{t}_{R_G} + \epsilon, t_1), \hat{t}_{R_G}]^\top & \text{if } \hat{t}_{R_G} < 1 \\ [t_1, \max(t_1, t_2)]^\top & \text{otherwise.} \end{cases} \quad (10)$$

where ϵ is an arbitrarily small positive number.

The proof is in Appendix 4.

The bar plot in Figure 4(a) shows an example for the Gödel t-conorm with four literals. The minimal refined vector is represented with the orange boxes, while the initial and refinement values of the entire formula are represented as a blue and purple line respectively. Here, our goal is to increase the value of the t-conorm, i.e., the maximum value. Increasing other literals up to \hat{t}_φ would require longer orange bars and bigger values for the L_p norm. Figure 4(b) represents when multiple literals have the largest truth value. Here, only one should be increased². Finally, Figure 4(c) shows the refined vector for the

²In our experiments, we choose randomly.

Gödel t-norm. Since the smallest truth value should be at least \hat{t}_φ , we simply ensure all truth values are at least \hat{t}_φ .

Our results are closely related to that of [14], which considers hard constraints, i.e., $\hat{t}_\varphi = 1$. In the hierarchical multi-label classification setting, the authors introduce an output layer that ensures predictions satisfy a set of hierarchy constraints. This layer corresponds to applications of the minimal refinement function for the Gödel implication with $\hat{t}_{RG} = 1$. Furthermore, [14] introduces C-HMCNN(h). This method considers an output layer that ensures predictions satisfy background knowledge expressed in a stratified normal logic program. The authors introduce an iterative algorithm that computes the minimal solution for such programs. This algorithm is related to that of ILR in Section 5. However, their formalization differs somewhat from ours, and future work could study whether these results also hold for our formalization of minimal refinement functions and if they can be extended to any value of \hat{t}_φ . Finally, [14] introduces a loss function that compensates for gradient bias introduced by the constrained output layer.

7.2.2 Łukasiewicz t-norm

In this section, we derive minimal refinement functions for the Łukasiewicz t-norm and t-conorm, for the family of p -norms. We will start using the following notation here: \mathbf{t}^\uparrow refers to the truth values t_i sorted in ascending order, while \mathbf{t}^\downarrow refers to the truth values sorted in descending order.

Proposition 5. *Let $\hat{t}_{T_L} \in [0, \max(\|\mathbf{c}\|_1 - (m-1), 0)]$ and define $\lambda_K = \frac{\hat{t}_{T_L} + m + K - 1 - \|\mathbf{c}\|_1 - \sum_{i=1}^K t_i^\uparrow}{K}$. Let K^* be the largest integer $1 \leq K \leq n$ such that $\lambda_K < 1 - t_K^\uparrow$. Then the minimal refinement vector of the Łukasiewicz t-norm is*

$$\rho_{T_L}^*(\mathbf{t}, \hat{t}_{T_L})_i = \begin{cases} t_i + \lambda_{K^*} & \text{if } \hat{t}_{T_L} > T_L(\mathbf{t}) \text{ and } t_i \leq t_{K^*}^\uparrow, \\ 1 & \text{if } \hat{t}_{T_L} > T_L(\mathbf{t}) \text{ and } t_i > t_{K^*}^\uparrow, \\ t_i - \frac{\max(\|\mathbf{t}\|_1 + \|\mathbf{c}\|_1 + 1 - n - \hat{t}_{T_L}, 0)}{n} & \text{otherwise.} \end{cases} \quad (11)$$

Let $\hat{t}_{S_L} \in [\min(\|\mathbf{c}\|_1, 1), 1]$ and define $\lambda_K = \frac{\|\mathbf{t}\|_1 + \|\mathbf{c}\|_1 - \hat{t}_{S_L}}{K}$. Let K^* be the largest integer $1 \leq K \leq n$ such that $\lambda_K < t_K^\downarrow$. Then the minimal refinement function of the Łukasiewicz t-conorm is

$$\rho_{S_L}^*(\mathbf{t}, \hat{t}_{S_L})_i = \begin{cases} t_i + \frac{\max(\hat{t}_{S_L} - \|\mathbf{t}\|_1 - \|\mathbf{c}\|_1, 0)}{n} & \text{if } \hat{t}_{S_L} > S_L(\mathbf{t}), \\ t_i - \lambda_{K^*} & \text{if } \hat{t}_{S_L} < S_L(\mathbf{t}) \text{ and } t_i \geq t_{K^*}^\downarrow, \\ 0 & \text{otherwise.} \end{cases} \quad (12)$$

Proof This follows from Propositions 1, 12 and 13, see Appendix A.2.1 and A.2.2. \square

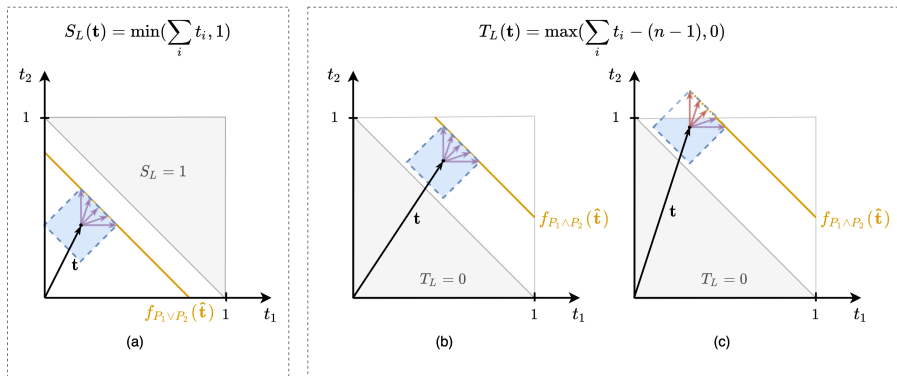


Fig. 5 Lukasiewicz minimal refinement functions. The orange line corresponds to the contour line of the S_L and T_L at the value \hat{t}_φ . Dotted blue circumference corresponds to a set of points at an equal distance from \mathbf{t} . (a) t-conorm; (b) t-norm; (c) t-norm in the limit case.

Although slightly obfuscated, these refinement functions simply increase each of the literals equally, while properly dealing with constraints on the truth values. We explain this using Figure 5, where the optimal solution corresponds to a vector that, from the original truth values \mathbf{t} , is perpendicular to the contour line of the operator at the value \hat{t}_φ . Moreover, the figure also provides some intuition for our proofs. The stationary points of the Lagrangian correspond to the points where the constraint function (blue circumference) tangentially touches the contour line of the refined value (orange line).

The change applied by the refinement function is proportional to the refinement value \hat{t} . Computing these refinement functions requires finding K^* , which can be done efficiently in log-linear time using a sort on the input truth values and a binary search.

The residuum of the Lukasiewicz t-norm is equal to its S-implication formed using $S_L(1 - a, c)$, and so its minimal refinement function can be found using Proposition 2.

The Lukasiewicz logic is unique in containing large convex and concave fragments [13]. In particular, any CNF formula interpreted using the weak conjunction (Gödel t-norm) and Lukasiewicz t-conorm is concave, allowing for efficient maximization using a quadratic program of a slightly relaxed variant of the problem in Equation 7. [13] studies this property in a setting similar to ours in the context of collective classification. Future work could study using this convex fragment to find minimal refinement functions for more complex formulas.

7.2.3 Product t-norm

To present the three basic t-norms together, we give the closed-form refinement function for the product t-norm with the L1 norm. Our proof is a special case of the general results on a large class of t-norms we will discuss in Section 7. In particular, the product t-norm is a strict, Schur-concave t-norm with an

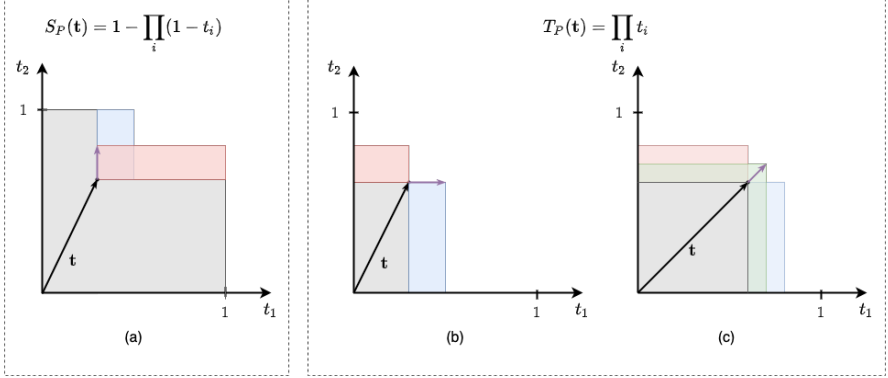


Fig. 6 Product minimal refinement functions. The grey areas represent the truth value of the operator associated with the initial vector \mathbf{t} . Red and blue areas represent the refined values when increasing a single literal. (a) t-conorm; (b) t-norm; (c) t-norm when multiple literals have same truth value. The green area represents the improvement obtained by increasing both literals equally.

additive generator. It is an example of a t-norm for which we can find a closed-form refinement function for the L1 norm using Propositions 15 and 1. First, we show the minimal refinement function for the product t-norm.

$$\rho_{T_P}^*(\mathbf{t}, \hat{t}_{T_P})_i = \begin{cases} n^{-K^*} \sqrt{\frac{\hat{t}_{T_P}}{\prod_{j=1}^{K^*} t_j^\downarrow \prod_{j=1}^m C_j}} & \text{if } T_P(\mathbf{t}, \mathbf{c}) > \hat{t}_{T_P} \text{ and } t_i \leq t_{K^*+1}^\downarrow, \\ \sqrt{\frac{\hat{t}_{T_P}}{\prod_{j \neq i} t_j^\downarrow \prod_{i=1}^m C_i}} & \text{if } T_P(\mathbf{t}, \mathbf{c}) < \hat{t}_{T_P} \text{ and } i = \arg \min_{j=1}^n t_j, \\ t_i & \text{otherwise.} \end{cases} \quad (13)$$

Next, we present the result for the product t-conorm:

$$\rho_{S_P}^*(\mathbf{t}, \hat{t}_{S_P})_i = \begin{cases} 1 - \sqrt{\frac{1 - \hat{t}_{S_P}}{\prod_{j \neq i} 1 - t_j^\downarrow \prod_{i=1}^m 1 - C_i}} & \text{if } S_P(\mathbf{t}, \mathbf{c}) < \hat{t}_{S_P} \text{ and } i = \arg \min_{j=1}^n t_j, \\ 1 - n^{-K^*} \sqrt{\frac{1 - \hat{t}_{S_P}}{\prod_{j=1}^{K^*} 1 - t_j^\downarrow \prod_{j=1}^m 1 - C_j}} & \text{if } S_P(\mathbf{t}, \mathbf{c}) > \hat{t}_{S_P} \text{ and } t_i \leq t_{K^*+1}^\downarrow, \\ t_i & \text{otherwise.} \end{cases} \quad (14)$$

This refined function increases all the literals smaller than a certain threshold up to the threshold itself, where we assume \hat{t}_{T_P} is greater than the initial truth value. In fact, like the other t-norms in the class discussed in Section 7, it is similar to the Gödel t-norm in that it increases all literals above some threshold to the same value. Similarly, the refinement function for the t-conorm increases the highest literal. Figure 6 gives an intuition behind this behaviour.

Finally, the residuum minimal refinement function can be found with $\rho_{I_P}^*(t_1, t_2, \hat{t}_{I_P}) = [t_1, \frac{\hat{t}_{I_P}}{t_1}]^\top$.

We also studied the minimal refinement function for the L2 norm, but concluded that the result is a 2 n th degree polynomial with no simple closed-form solutions. For details, see Appendix D.

8 A general class of t-norms with analytical minimal refinement functions

In this section, we will introduce and discuss a general class of t-norms that have analytic solutions to the problem in Equation 7 in order to find their corresponding minimal refinement functions. We can find those for the t-norm, t-conorm, and the residuum.

8.1 Background on t-norms

To be able to properly discuss this class of t-norms, we first have to provide some more background on the theory of t-norms.

8.1.1 Additive generators

The study of t-norms frequently involves the study of their *additive generator* [22, 23], which are univariate functions that can be used to construct t-norms, t-conorms and residuums.

Definition 7. A function $g : [0, 1] \rightarrow [0, \infty]$ such that $g(1) = 0$ is an *additive generator* if it is strictly decreasing, right-continuous at 0, and if for all $t_1, t_2 \in [0, 1]$, $g(t_1) + g(t_2)$ is either in the range of g or in $[g(0^+), \infty)$.

Theorem 1. *If g is an additive generator, then the function $T : [0, 1]^n \rightarrow [0, 1]$ defined as*

$$T(\mathbf{t}) = g^{-1}(\min(g(0^+), \sum_{i=1}^n g(t_i))) \quad (15)$$

is a t-norm.

Using Equation 15, the function g acts like an invertible function. It transforms truth values into a new space that can be seen as measuring ‘untruthfulness’. $\sum_{i=1}^n g(t_i)$ can be seen as a measure of ‘untruth’ of the conjunction. T-norms constructed in this way are necessarily Archimedean, and each continuous Archimedean t-norm has an additive generator. T_P , T_L and T_D have an additive generator, but T_G and T_N do not. Furthermore, if $g(0^+) = \infty$, T is strict and we find $T(\mathbf{t}) = g^{-1}(\sum_{i=1}^n g(t_i))$. The residuum constructed from continuous t-norms with an additive generator can be computed using $g^{-1}(\max(g(c) - g(a), 0))$ [20].

8.1.2 Schur-concave t-norms

We will frequently consider the class of Schur-concave t-norms, with their dual t-conorms and residuums formed from these Schur-concave t-norms. We denote

with \mathbf{t}^\downarrow the truth vector \mathbf{t} sorted in descending order, and with \mathbf{t}^\uparrow as \mathbf{t} sorted in ascending order.

Definition 8. A vector $\mathbf{t} \in \mathbb{R}^n$ is said to *majorize* another vector $\mathbf{u} \in \mathbb{R}^n$, denoted $\mathbf{t} \succ \mathbf{u}$, if $\sum_{i=1}^n t_i = \sum_{i=1}^n u_i$ and if for each $i \in \{1, \dots, n\}$ it holds that $\sum_{j=1}^i t_j^\downarrow \geq \sum_{j=1}^i u_j^\downarrow$.

Definition 9. A function $[0, 1]^n \rightarrow [0, 1]$ is called *Schur-convex* if for all $\mathbf{t}, \mathbf{u} \in [0, 1]^n$, $\mathbf{t} \succ \mathbf{u}$ implies that $f(\mathbf{t}) \geq f(\mathbf{u})$. Similarly, a *Schur-concave* function has that $\mathbf{t} \succ \mathbf{u}$ implies that $f(\mathbf{t}) \leq f(\mathbf{u})$.

The dual t-conorm of a Schur-concave t-norm is Schur-convex. The three basic and continuous t-norms T_G , T_P and T_L are Schur-concave. There are also non-continuous Schur-concave t-norms, such as the Nilpotent minimum [30, 32]. The drastic t-norm is an example of a t-norm that is not Schur-concave [30]. This class includes all quasiconcave t-norms since all symmetric quasiconcave functions are also Schur-concave [26, p98 C.3]. Therefore, this class constitutes a significant class of relevant t-norms. For a more precise characterization of Schur-concave t-norms, see [2, 30].

8.2 Minimal refinement functions for Schur-concave t-norms

We now have the background to discuss several useful and interesting results on Schur-concave t-norms. First, we present two results that characterize Schur-concave minimal refinement functions. We use the notion of “strictly cone-increasing” functions here that is discussed in Appendix B.1.

Theorem 2. *Let T be a Schur-concave t-norm that is strictly cone-increasing at \hat{t}_T and let $\|\cdot\|$ be a strict norm. Then there is a minimal refined vector \mathbf{t}^* for \mathbf{t} and \hat{t}_T such that whenever $t_i > t_j$, then $t^*_i - t_i \leq t^*_j - t_j$.*

For proof, see Appendix C.1. We note that we can make this argument in the other direction to show that any Schur-convex t-conorm will have a minimal refined vector such that $t_i > t_j$ implies $t^*_i \geq t^*_j$. Furthermore, if we know that a t-norm has a unique minimal refinement function, we can use this theorem to infer a useful ordering on how it changes the truth values.

Next, we will consider the L1 norm $\sum_{i=1}^n |\hat{t}_i - t_i|$, for which we can find general solutions for the t-norm, t-conorm and R-implication when the t-norm is Schur-concave.

Proposition 6. *Let $\mathbf{t} \in [0, 1]^n$ and let T be a Schur-concave t-norm that is strictly cone-increasing at $\hat{t}_T \in [T(\mathbf{t}, \mathbf{c}), \max_T]$. Then there is a value $\lambda \in [0, 1]$*

such that the vector \mathbf{t}^* ,

$$t^*_i = \begin{cases} \lambda, & \text{if } t_i < \lambda, \\ t_i, & \text{otherwise,} \end{cases} \quad (16)$$

is a minimal refined vector for T and the L1 norm at \mathbf{t} and \hat{t}_T .

For proof, see Appendix C.2. We found this result rather surprising: It is optimal for a large class of t-norms and the L1 norm to increase the lower truth values to some value λ . In this sense, these solutions are very similar to that of the Gödel refinement functions. The value of λ depends on the choice of t-norm and $T(\mathbf{t}^*, \mathbf{c})$ is a non-decreasing function of λ . We show in Section 8.3 how to compute these.

We have a similar result, proof in the end of Appendix C.2, for the refinement functions of Schur-convex t-conorms. This proposition shows that, under the L1 norm, it is optimal to increase only the largest literal, just like with the Gödel t-norm.

Proposition 7. *Let $\mathbf{t} \in [0, 1]^n$ and let S be a Schur-convex t-conorm that is strictly cone-increasing at $\hat{t}_S \in [S(\mathbf{t}, \mathbf{c}), 1]$. Then there is a value $\lambda \in [0, 1]$ such that the vector \mathbf{t}^* ,*

$$t^*_i = \begin{cases} \lambda & \text{if } i = \arg \max_{i \in D} t_i, \\ t_i, & \text{otherwise,} \end{cases} \quad (17)$$

is a minimal refined vector for S and the L1 norm at \mathbf{t} and \hat{t}_S .

8.3 Closed forms using Additive Generators

Where the previous section gives general results on the form or “shape” of minimal refinement functions for t-norms and t-conorms under the L1 norm, we still need to figure out what the value of λ is for a particular \hat{t}_φ . Luckily, additive generators will do the job here.

Proposition 8. *Let T be a Schur-concave t-norm with additive generator g and let $0 < \hat{t}_T \in [T(\mathbf{t}, \mathbf{c}), \max_T]$. Let $K \in \{0, \dots, n - 1\}$ denote the number of truth values such that $t^*_i = t_i$ in Equation 28. Then using*

$$\lambda_K = g^{-1} \left(\frac{1}{n - K} \left(g(\hat{t}_T) - \sum_{i=1}^K g(t_i^\dagger) - \sum_{i=1}^m g(C_i) \right) \right) \quad (18)$$

in Equation 28 gives $T(\mathbf{t}^*, \mathbf{c}) = \hat{t}_T$ if $\mathbf{t}^* \in [0, 1]^n$.

See Appendix C.2 for a proof. $g(\hat{t}_T)$ can be seen as the ‘untruth’-value in g -space that \mathbf{t}^* should attain. Since we have $n - K$ truth values that we can move freely, we need to make sure that their ‘untruth’-value in g -space is

$g(\hat{t}_T)/(n - K)$. However, we also need to handle the truth values we cannot change freely, which is why those are subtracted from $g(\hat{t}_T)$.

We should note that this does not yet give a procedure for computing the correct $K \in \{0, \dots, n - 1\}$. The intuition here is that we should find an K such that $t_i \geq \lambda_K$ for the K largest values, and $t_i < \lambda_K$ for the remaining $n - K$. Like with computing the K^* for the refinement function for the Łukasiewicz t-norm (Section 7.2.2), we can do this in logarithmic time after sorting \mathbf{t} , but we choose to compute λ_K for each $K \in \{0, n - 1\}$ in parallel.

We can similarly find a closed form for the t-conorms:

$$\lambda = 1 - g^{-1} \left(g(1 - \hat{t}_S) - \sum_{i \neq j} g(1 - t_i) - \sum_{i=1}^m g(1 - C_i) \right) \quad (19)$$

Proposition 9. *Let $t_1, t_2 \in [0, 1]$ and let T be a strict Schur-concave t-norm with additive generator g . Consider its residuum $R(t_1, t_2) = \sup\{z | T(t_1, z) \leq t_2\}$ that is strictly cone-increasing at $0 < \hat{t}_R \in [R(t_1, t_2), \max_R]$. Then there is a value $\lambda \in [0, 1]$ such that $\mathbf{t}^* = [t_1, g^{-1}(g(\hat{t}_R) + g(t_1))]^\top$ is a minimal refined vector for R and the L1 norm at \mathbf{t} and t .*

Here, we find that for this class of residuums, increasing the consequent (the second argument of the implication) is minimal for the L1 norm. This update reflects modus ponens reasoning: When the antecedent is true, increase the consequent. As we have argued in [32], this could cause issues in many machine learning setups: Consider the modus tollens correction instead decreases the antecedent. For common-sense knowledge, this is more likely to reflect the true state of the world.

9 Experiments

We performed experiments on two tasks. The first one does not involve learning. Instead, we aim to solve SAT problems. This experiment allows assessing whether ILR can enforce complex and unstructured knowledge. The second experiment is on the MNIST Addition task [25] to test ILR in a neuro-symbolic setting and assess its ability to learn from data.

9.1 Experiments on 3SAT problems

With this experiments, our goal is to find out how quickly ILR finds a refined vector and how minimal this vector is. We test this on formulas of varying complexity to analyze for what problems each algorithm performs well³.

³Code available at <https://github.com/DanieleAlessandro/IterativeLocalRefinement>

9.1.1 Setup

We perform experiments on SATLIB [18], a library of randomly generated 3SAT problems. 3SAT problems are formulas in the form $\bigwedge_{i=1}^c \bigvee_{j=1}^3 l_{ij}$, where l_{ij} is a literal that is either P_k or $\neg P_k$ and where $P_k \in \{P_1, \dots, P_n\}$ is an input proposition. In particular, we consider uf20-91 of satisfiable 3SAT problems with $n = 20$ propositions and $c = 91$ disjunctive clauses. For this, we select the refined value \hat{t}_φ to be 1. We also experiment with $\hat{t}_\varphi \in \{0.3, 0.5\}$ in Appendix E. We uniformly generate initial truth values for the propositions $\mathbf{t} \in [0, 1]^d$ ⁴. To allow experimenting with formulas of varying complexity, we introduce a simplified version of the task which uses only the first 20 clauses.

We compare ILR with a gradient descent baseline described in Section 9.1.2 using three metrics. The first is speed: How many iterations does it take for each algorithm to converge? Since both algorithms have similar computational complexities, we will use the number of iterations for this. The second is satisfaction: Is the algorithm able to find a solution with truth value \hat{t}_φ ? Finally, we consider minimality: How close to the original prediction is the refined vector $\hat{\mathbf{t}}$? Note that the refinement function for the product logic is only optimal for the L1 norm, while for Gödel and Łukasiewicz, the refinement function is optimal for all L_p norms, including L1. Moreover, the results of L1 and L2 are very similar. Therefore, we use the L1 as a metric for minimality for each t-norm.

9.1.2 Gradient descent baseline

We compare ILR to gradient descent with the following loss function

$$\mathcal{L}(\hat{\mathbf{z}}, \mathbf{t}, \hat{t}_\varphi) = \|f_\varphi(\sigma(\hat{\mathbf{z}})) - \hat{t}_\varphi\|_2 + \alpha \|\sigma(\hat{\mathbf{z}}) - \mathbf{t}\|_p. \quad (20)$$

Here $\hat{\mathbf{t}} = \sigma(\hat{\mathbf{z}})$ is a real-valued vector $\hat{\mathbf{z}} \in \mathbb{R}^n$ transformed to $\hat{\mathbf{t}} \in [0, 1]^n$ using the sigmoid function σ to ensure the values of $\hat{\mathbf{t}}$ remain in $[0, 1]^n$ during gradient descent. The first term minimizes the distance between the current truth value of the formula φ and the refinement value, while the second term is a regularization term that minimizes the distance between the refined vector and the original truth value \mathbf{t} in the L_p norm. α is a hyperparameter that trades off the importance of this regularization term.

This method for finding refined vectors is very similar to the collective classification method introduced in SBR [9, 29]. The main difference is in the L_p norms chosen, as we use squared error for the first term instead of the L1 norm. Gradient descent is a steepest descent method that take steps minimizing the L2 norm. Therefore, it can also be seen as a method for finding minimal refinement functions given the L2 norm. The corresponding steepest descent method for the L1 norm is the coordinate descent algorithm. Future work could compare how coordinate descent performs for finding minimal refinement functions for the L1 norm. We suspect it will be much slower than gradient descent-based methods as it can only change a single truth value each iteration.

⁴Each run used the same initial value for each algorithm to have a fair comparison.

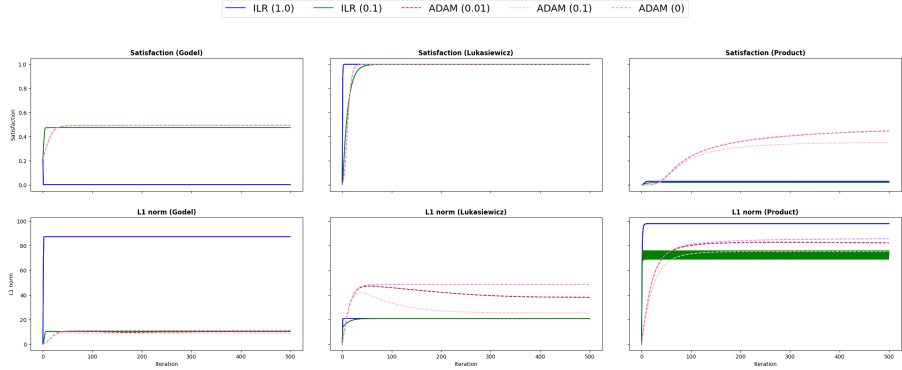


Fig. 7 Comparison of ILR with ADAM on uf20-91 in SATLIB. Refined value 1.0.. The x axis corresponds to the number of iterations, while the y axis is the value of \hat{t}_φ in the first row of the grid, and the L1 norm in the second row.

We found that ADAM [21] significantly outperformed standard gradient descent in all metrics, and we chose to use it throughout our experiments. Furthermore, inspired by the analysis of the derivatives of aggregation operators in [32], we slightly change the formulation of the loss function for the Łukasiewicz t-norm and product t-norm. The Łukasiewicz t-norm will have precisely zero gradients for most of its domain. Therefore, we remove the max operator when evaluating the \wedge in the SAT formula so it has nonzero gradients. For the product t-norm, the gradient will also approach 0 because of the large set of numbers between $[0, 1]$ that it multiplies. As suggested by [32], we instead optimize the logarithm of the product t-norm:

$$\mathcal{L}_P(\hat{\mathbf{z}}, \mathbf{t}, \hat{t}_\varphi) = \left\| \sum_{i=1}^c \log f_{\sqrt[3]{j=1}}(\sigma(\mathbf{t})) - \log \hat{t}_\varphi \right\|_2 + \alpha \|\sigma(\hat{\mathbf{z}}) - \mathbf{t}\|_1.$$

9.1.3 Results

In Figure 7 we show the results obtained by ILR and ADAM on the three t-norms (one for each column of the grid). We observe that ILR with schedule parameter $\alpha = 0.1$ has a smoother plot compared to ILR with $\alpha = 1.0$, which converges faster: In our experiments, the number of steps until convergence was always between 2 and 5. For both values of the scheduling parameters, ILR outperforms ADAM in terms of convergence speed.

When comparing satisfaction and minimality, the behavior differs based on the t-norm used. In the case of Łukasiewicz, all methods find feasible solutions to the optimization problem. Furthermore, in terms of minimality (i.e., L1 norm), ILR finds better solutions than ADAM.

For the Gödel logic no method is capable of reaching a feasible solution. Here, ILR with schedule parameter $\alpha = 1$ performs very poorly, obtaining worse solutions than the original truth values. On the other hand, with $\alpha = 0.1$, it performs as well as ADAM for both metrics but with faster convergence.

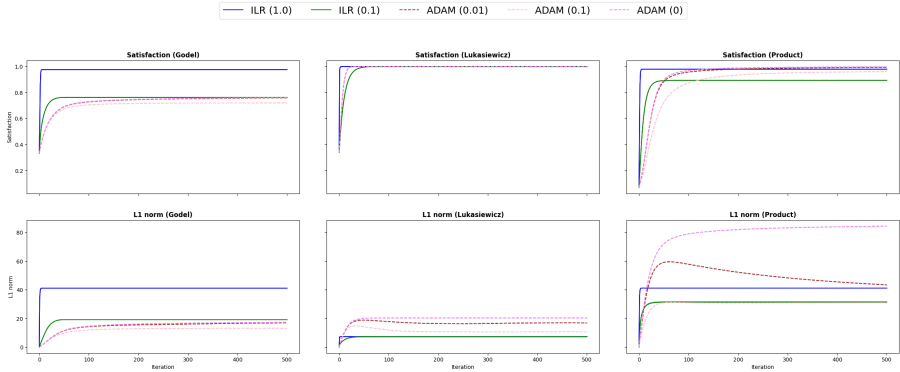


Fig. 8 Comparison of ILR with ADAM on the uf20-91 with 20 clauses. Target value 1.0.

Finally, for the product logic, ILR fails to increase the satisfaction of the formula to the refined value. However, ADAM can find much better solutions, getting the average truth value to around 0.5. Still, it is far from reaching a feasible solution. Nonetheless, we recommend using ADAM for complicated formulas in the product logic.

However, we argue that in the context of Neural-Symbolic Integration, the provided knowledge is usually relatively easy to satisfy. With 91 clauses, there are few satisfying solutions in this space of 2^{21} possible binary solutions. However, background knowledge usually does not constrain the space of possible solutions as heavily as this. For this reason, we propose a simplified formula, where we only use 20 out of 91 clauses. Figure 8 shows the results for this setting. We see that ILR with no scheduling ($\alpha = 1$) finds feasible solutions for all t-norms. ILR finds solutions for the Gödel t-norm where ADAM cannot find any, while for Łukasiewicz and product, it finds solutions in much fewer iterations and with a lower L1 norm. Hence, we argue that for knowledge bases that are less constraining, ILR without scheduling is the best choice.

9.2 Experiments on MNIST Addition

The experiments on the SATLIB benchmark show how well ILR can enforce knowledge in highly constrained settings. However, as already mentioned, in neuro-symbolic AI, the background knowledge is typically much simpler. SAT benchmarks often only have a few solutions, heavily limiting what predictions the neural network can make. Moreover, previous experiments only tested ILR where initial truth vectors are random, and we did not have any neural networks or learning.

To evaluate the performance of ILR in neuro-symbolic settings, we implemented the architecture of Figure 3. Here, the task is to learn a classifier for handwritten digits while only receiving supervision on the sums of pairs of digits.

	30000	3000
DeepProbLog [25]	97.20 \pm 0.45	92.18 \pm 1.57
LTN [3]	96.78 \pm 0.5	92.15 \pm 0.75
ILR	96.67 \pm 0.45	93.38 \pm 1.70

Table 2 Results on the MNIST addition task. We report the accuracy of predicting the sum (in %) on the test set with 30000 and 3000 samples. DeepProbLog results are taken from [3]. LTN results have been obtained by replicating the experiments of [3].

9.2.1 Setup

We follow the architecture of Figure 3. We use the neural network proposed by [25], which is a network composed of two convolutional layers, followed by a MaxPool layer, followed by a fully connected layer with ReLU activation function and a fully connected layer with softmax activation. We use the Gödel t-norm and corresponding minimal refinement functions. Note that Gödel implication can only increase the consequent and can never decrease the antecedents. For this reason, ILR converges in a single step.

We set both α and target value \hat{t} to one, meaning that we ask ILR to make the entire formula completely satisfied in one step. We use the ADAM optimizer and a learning rate of 0.01, with the cross-entropy loss function. However, since the outputs of the ILR step do not sum to one, we cannot directly apply it to the refined vector ILR computes. To overcome this issue, we add a logarithm followed by a softmax as the last layers of the model. If the sum of the refined vector is one, the composition of the logarithm and softmax functions corresponds to the identity function. Moreover, these two layers are monotonic increasing functions and preserve the order of the refined vector.

We use the dataset defined in [25] with 30000 samples, and also run the experiment using only 10% of the dataset (3000 samples). We run ILR for 5 epochs on the complete dataset, and 30 epochs on the small one. We repeat this experiment 10 times. We are interested in the accuracy obtained in the test set for the addition task. We ran the experiments on a MacBook Pro (2016) with a 3,3 GHz Dual-Core Intel Core i7.

9.2.2 Results

ILR can efficiently learn to predict the sum, reaching results similar to the state of the art, requiring on average 30 seconds per epoch. However, sometimes ILR got stuck in a local minimum during training, where the accuracy reached was close to 50%. It is worth noticing that LTN suffers from the same problem [3], with results strongly dependent on the initialization of the parameters. To better understand this local minimum, we analyzed the confusion matrix. Figure 9 shows one of the confusion matrices for a model stuck in the local minimum: the CNN recognizes each digit either as the correct digit minus one or plus one. Then, our model obtains the correct prediction in close to 50% of the cases. For example, suppose the digits are a 3 and a 5. The 3 is classified either as either a 2 or a 4, while the 5 is classified as a 4 or a 6.

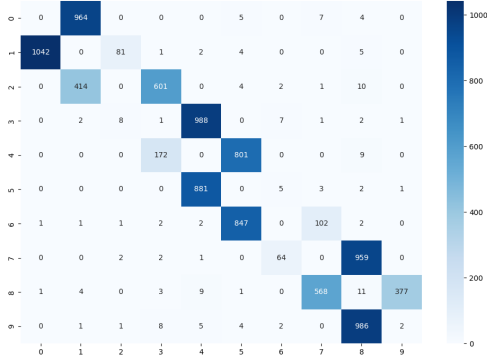


Fig. 9 Confusion matrix on the MNIST classification for a local minimum

If the model predicts 2 and 6 or 4 and 4, it returns the correct sum (8), otherwise, it does not. We believe that in these local minima there is no way for the model to change the digit predictions without increasing the loss, and the model remains stuck in the local minimum.

Table 2 shows the results in terms of accuracy of ILR, LTN [3] and Deep-Problog [25]. To calculate the accuracy, we follow [3] and select only the models that do not stop in the local minimum. Notice that this problem is very rare for ILR (once every 30 runs) and happens more frequently with LTN (once every 5 runs).

10 Conclusion and Future Work

We analytically studied a large class of minimal fuzzy refinement functions. We used refinement functions to construct ILR, an efficient algorithm for general formulas. Another benefit of these analytical results is to get a good intuition into what kind of corrections are done by each t-norm. In our experimental evaluation of this algorithm, we found that our algorithm converges much faster and often finds better solutions than the baseline ADAM, especially for problems that are less constraining. However, for complicated formulas and the product logic, we conclude ADAM finds better results. Finally, we assess ILR on the MNIST Addition task and show it can be combined with a neural network, providing results similar to two of the most prominent methods for neuro-symbolic AI.

There is a lot of opportunity for future work on refinement functions. We will study how the refinement functions induced by different t-norms perform in practical neuro-symbolic integration settings. On the theoretical side, possible future work could be considering analytical refinement functions for certain classes of complex formulas. Furthermore, there are many classes of t-norms and norms for which finding analytical refinement functions is an open problem. Another promising avenue for research is designing specialized loss functions that handle biases in the gradients arising from combining constrained output layers with cross-entropy loss functions [14]. We also want to

highlight the possibility of extending the work on fuzzy refinement functions to probabilistic refinement functions, using a notion of minimality such as the KL-divergence.

Acknowledgements

Alessandro Daniele and Emile van Krieken are involved in a HumaneAI Micro-project. HumaneAI received funding from the European Union’s Horizon 2020 research and innovation program under grant agreement No 761758.

References

- [1] K. Ahmed, S. Teso, K.-W. Chang, G. V. den Broeck, and A. Vergari. Semantic Probabilistic Layers for Neuro-Symbolic Learning. In *The 5th Workshop on Tractable Probabilistic Modeling*, July 2022.
- [2] C. Alsina. On Schur-Concave t-Norms and Triangle Functions. In W. Walter, editor, *General Inequalities 4: In Memoriam Edwin F. Beckenbach 4th International Conference on General Inequalities, Oberwolfach, May 8–14, 1983*, pages 241–248. Birkhäuser, Basel, 1984. ISBN 978-3-0348-6259-2. doi: 10.1007/978-3-0348-6259-2_22.
- [3] S. Badreddine, A. d’Avila Garcez, L. Serafini, and M. Spranger. Logic Tensor Networks. *Artificial Intelligence*, 303:103649, Feb. 2022. ISSN 0004-3702. doi: 10.1016/j.artint.2021.103649.
- [4] T. Calvo, A. Kolesárová, M. Komorníková, and R. Mesiar. Aggregation operators: Properties, classes and construction methods. In T. Calvo, G. Mayor, and R. Mesiar, editors, *Aggregation Operators: New Trends and Applications*, pages 3–104. Physica-Verlag HD, Heidelberg, 2002. ISBN 978-3-7908-1787-4.
- [5] A. Chowdhery, S. Narang, J. Devlin, M. Bosma, G. Mishra, A. Roberts, P. Barham, H. W. Chung, C. Sutton, S. Gehrmann, P. Schuh, K. Shi, S. Tsvyashchenko, J. Maynez, A. Rao, P. Barnes, Y. Tay, N. Shazeer, V. Prabhakaran, E. Reif, N. Du, B. Hutchinson, R. Pope, J. Bradbury, J. Austin, M. Isard, G. Gur-Ari, P. Yin, T. Duke, A. Levskaya, S. Ghemawat, S. Dev, H. Michalewski, X. Garcia, V. Misra, K. Robinson, L. Fedus, D. Zhou, D. Ippolito, D. Luan, H. Lim, B. Zoph, A. Spiridonov, R. Sepassi, D. Dohan, S. Agrawal, M. Omernick, A. M. Dai, T. S. Pili-lai, M. Pellat, A. Lewkowycz, E. Moreira, R. Child, O. Polozov, K. Lee, Z. Zhou, X. Wang, B. Saeta, M. Diaz, O. Firat, M. Catasta, J. Wei, K. Meier-Hellstern, D. Eck, J. Dean, S. Petrov, and N. Fiedel. PaLM: Scaling Language Modeling with Pathways. *arXiv:2204.02311 [cs]*, Apr. 2022.

- [6] F. H. Clarke, R. J. Stern, and P. R. Wolenski. Subgradient Criteria for Monotonicity, The Lipschitz Condition, and Convexity. *Canadian Journal of Mathematics*, 45(6):1167–1183, Dec. 1993. ISSN 0008-414X, 1496-4279. doi: 10.4153/CJM-1993-065-x.
- [7] A. Daniele and L. Serafini. Knowledge enhanced neural networks. In A. C. Nayak and A. Sharma, editors, *PRICAI 2019: Trends in Artificial Intelligence*, pages 542–554, Cham, 2019. Springer International Publishing. ISBN 978-3-030-29908-8.
- [8] A. Daniele and L. Serafini. Knowledge enhanced neural networks for relational domains. *arXiv preprint arXiv:2205.15762*, 2022.
- [9] M. Diligenti, M. Gori, and C. Sacca. Semantic-based regularization for learning and inference. *Artificial Intelligence*, 244:143–165, 2017.
- [10] I. Donadello, L. Serafini, and A. d’Avila Garcez. Logic tensor networks for semantic image interpretation. In *IJCAI International Joint Conference on Artificial Intelligence*, pages 1596—1602, 2017.
- [11] P. Dragone, S. Teso, and A. Passerini. Neuro-Symbolic Constraint Programming for Structured Prediction. page 9.
- [12] M. Fischer, M. Balunovic, D. Drachsler-Cohen, T. Gehr, C. Zhang, and M. Vechev. DL2: Training and Querying Neural Networks with Logic. page 11.
- [13] F. Giannini, M. Diligenti, M. Gori, and M. Maggini. On a Convex Logic Fragment for Learning and Reasoning. *IEEE Transactions on Fuzzy Systems*, 27(7):1407–1416, July 2019. ISSN 1063-6706, 1941-0034. doi: 10.1109/TFUZZ.2018.2879627. Comment: Accepted in IEEE Transactions on Fuzzy Systems.
- [14] E. Giunchiglia and T. Lukasiewicz. Multi-Label Classification Neural Networks with Hard Logical Constraints, Mar. 2021. Comment: arXiv admin note: text overlap with arXiv:2010.10151.
- [15] E. Giunchiglia, M. Stoian, S. Khan, F. Cuzzolin, and T. Lukasiewicz. ROAD-R: The Autonomous Driving Dataset with Logical Requirements. June 2022.
- [16] E. Giunchiglia, M. C. Stoian, and T. Lukasiewicz. Deep Learning with Logical Constraints, May 2022. Comment: Survey paper. IJCAI 2022.
- [17] N. Hoernle, R. M. Karampatsis, V. Belle, and K. Gal. MultiplexNet: Towards Fully Satisfied Logical Constraints in Neural Networks. *Proceedings of the AAAI Conference on Artificial Intelligence*, 36(5):5700–5709,

June 2022. ISSN 2374-3468, 2159-5399. doi: 10.1609/aaai.v36i5.20512.

- [18] H. H. Hoos. SATLIB : An online resource for research on SAT. pages 1–12, 2000.
- [19] W. R. Inc. *Mathematica, Version 12.0*. 2019. Champaign, IL, 2019.
- [20] B. Jayaram and M. Baczynski. *Fuzzy Implications*, volume 231. Springer, Berlin, Heidelberg, 2008. ISBN 978-3-540-69080-1. doi: 10.1007/978-3-540-69082-5.
- [21] D. P. Kingma and J. Ba. Adam: A Method for Stochastic Optimization. *arXiv:1412.6980 [cs]*, Jan. 2017. Comment: Published as a conference paper at the 3rd International Conference for Learning Representations, San Diego, 2015.
- [22] E. P. Klement, R. Mesiar, and E. Pap. Triangular norms. Position paper II: General constructions and parameterized families. *Fuzzy Sets and Systems*, 145(3):411–438, Aug. 2004. ISSN 01650114. doi: 10.1016/S0165-0114(03)00327-0.
- [23] E. P. Klement, R. Mesiar, and E. Pap. *Triangular Norms*, volume 8. Springer Science & Business Media, 2013.
- [24] Y. LeCun and C. Cortes. MNIST handwritten digit database. 2010.
- [25] R. Manhaeve, S. Dumančić, A. Kimmig, T. Demeester, and L. De Raedt. DeepProbLog: Neural probabilistic logic programming. In S. Bengio, H. M. Wallach, H. Larochelle, K. Grauman, N. Cesa-Bianchi, and R. Garnett, editors, *Advances in Neural Information Processing Systems 31: Annual Conference on Neural Information Processing Systems 2018, NeurIPS 2018, 3-8 December 2018, Montréal, Canada*, 2018.
- [26] A. W. Marshall, I. Olkin, and B. C. Arnold. Schur-Convex Functions. In A. W. Marshall, I. Olkin, and B. C. Arnold, editors, *Inequalities: Theory of Majorization and Its Applications*, pages 79–154. Springer, New York, NY, 2011. ISBN 978-0-387-68276-1. doi: 10.1007/978-0-387-68276-1.3.
- [27] A. Ramesh, P. Dhariwal, A. Nichol, C. Chu, and M. Chen. Hierarchical Text-Conditional Image Generation with CLIP Latents. *arXiv:2204.06125 [cs]*, Apr. 2022.
- [28] T. J. U. o. N. M. Ross. *Fuzzy Logic with Engineering Applications*. 2010. ISBN 978-0-470-74376-8. doi: 10.1002/9781119994374.
- [29] S. Roychowdhury, M. Diligenti, and M. Gori. Regularizing deep networks with prior knowledge: A constraint-based approach. *Knowledge-Based*

Systems, 222:106989, June 2021. ISSN 0950-7051. doi: 10.1016/j.knosys.2021.106989.

- [30] A. Takači. Schur-concave triangular norms: Characterization and application in pFCSP. *Fuzzy Sets and Systems. An International Journal in Information Science and Engineering*, 155(1):50–64, 2005.
- [31] H. A. Van Dyke, K. R. Vixie, and T. J. Asaki. Cone Monotonicity: Structure Theorem, Properties, and Comparisons to Other Notions of Monotonicity. *Abstract and Applied Analysis*, 2013:1–8, 2013. ISSN 1085-3375, 1687-0409. doi: 10.1155/2013/134751.
- [32] E. van Krieken, E. Acar, and F. van Harmelen. Analyzing differentiable fuzzy logic operators. *Artificial Intelligence*, 302:103602, 2022. ISSN 0004-3702. doi: 10.1016/j.artint.2021.103602.
- [33] P.-W. Wang, P. L. Donti, B. Wilder, and Z. Kolter. SATNet: Bridging deep learning and logical reasoning using a differentiable satisfiability solver. *arXiv:1905.12149 [cs, stat]*, May 2019. Comment: Accepted at ICML’19. The code can be found at <https://github.com/locuslab/satnet>.
- [34] J. Xu, Z. Zhang, T. Friedman, Y. Liang, and G. den Broeck. A semantic loss function for deep learning with symbolic knowledge. In J. Dy and A. Krause, editors, *Proceedings of the 35th International Conference on Machine Learning*, volume 80, pages 5502–5511, Stockholmssmässan, Stockholm Sweden, 2018. PMLR.
- [35] Z. Yang, J. Lee, and C. Park. Injecting Logical Constraints into Neural Networks via Straight-Through Estimators. page 27.

A Basic T-norms (Proofs)

A.1 Gödel t-norm minimal refined function proofs

A.1.1 Gödel t-norm

Proposition 10. *The minimal refinement function of the Gödel t-norm for $\hat{t}_{T_G} \in [T_G(\mathbf{t}, \mathbf{c}), \min_{i=1}^m C_i]$ is*

$$\rho_{T_G}^*(\mathbf{t}, \hat{t}_{T_G})_i = \begin{cases} \hat{t}_{T_G} & \text{if } t_i < \hat{t}_{T_G}, \\ t_i & \text{otherwise} \end{cases} \quad (21)$$

Proof Assume otherwise. Then there is a refined vector $\hat{\mathbf{t}}$ for T_G , $\mathbf{t} \in [0, 1]^n$ and $\hat{t}_{T_G} \in [T_G(\mathbf{t}), \min_{i=1}^m C_i]$ such that $\hat{\mathbf{t}} \neq \mathbf{t}^*$ while $\|\hat{\mathbf{t}} - \mathbf{t}\|_p < \|\mathbf{t}^* - \mathbf{t}\|_p$, where $\mathbf{t}^* = \rho_{T_G}^*(\mathbf{t}, \hat{t}_{T_G})$. Since $T_G(\hat{\mathbf{t}}) = \hat{t}_{T_G}$, for all $i \in \{1, \dots, n\}$, $\hat{t}_i \geq \hat{t}_{T_G}$ and so necessarily for all i such that $t_i < \hat{t}_{T_G}$, $\hat{t}_i \geq \hat{t}_{T_G}$. Since there is some i such that $\hat{t}_i \neq t_i$, either $t_i < \hat{t}_{T_G}$ and

then necessarily $\hat{t}_i > t^*_i$, or $\hat{t}_i \geq \hat{t}_{T_G}$ but $\hat{t}_i \neq t^*_i = t_i$. In either case, since $\|\cdot\|_p$ is strictly convex in each argument with minimum at \mathbf{t} , $\|\hat{\mathbf{t}} - \mathbf{t}\|_p > \|\mathbf{t}^* - \mathbf{t}\|_p$, hence $\hat{\mathbf{t}}$ could not have smaller norm. \square

A.1.2 Gödel t-conorm

A derivation for increasing the Gödel t-conorm was first presented in [7] and is adapted to our notation here:

Proposition 11. *The minimal refinement function of the Gödel t-conorm for $\hat{t}_{S_G} \in [S_G(\mathbf{t}, \mathbf{c}), 1]$ is*

$$\rho_{S_G}^*(\mathbf{t}, \hat{t}_{S_G})_i = \begin{cases} \hat{t}_{S_G} & \text{if } i = \arg \max_{j=1}^n t_j \\ t_i & \text{otherwise.} \end{cases} \quad (22)$$

A.1.3 Gödel Implication

We next present a proof for Proposition 4.

Proof First, assume $\hat{t}_{R_G} < 1$. To ensure $R_G(t_1, t_2) = \hat{t}_{R_G}$, we require $t_2 = \hat{t}_{R_G}$ as is clear from the definition. However, we also require $t_1 > \hat{t}_{R_G}$. If t_1 is already larger, we can leave it to ensure minimality. Otherwise, we require it to be at least infinitesimally bigger, that is $\hat{t}_{R_G} + \epsilon$.

Next, assume $\hat{t}_{R_G} = 1$. If $t_1 \leq t_2$, then the implication is already 1 and we do not need to revise anything. Otherwise, setting it equal to any value between t_2 and t_1 is minimal. \square

A.2 Łukasiewicz t-norm minimal refined function proofs

A.2.1 Łukasiewicz t-norm

Proposition 12. *Let $\hat{t}_{T_L} \in [T_L(\mathbf{t}, \mathbf{c}), \max(\|\mathbf{c}\|_1 - (m-1), 0)]$ and define $\lambda_K = \frac{\hat{t}_{T_L} + m + K - 1 - \|\mathbf{c}\|_1 - \sum_{i=1}^K t_i^\uparrow}{K}$. Let K^* be the largest integer $1 \leq K \leq |D|$ such that $\lambda_{K^*} < 1 - t_{K^*}^\uparrow$. Then the minimal refinement vector of the Łukasiewicz t-norm is*

$$\rho_{T_L}^*(\mathbf{t}, \hat{t}_{T_L})_i = \begin{cases} t_i + \lambda_{K^*} & \text{if } t_i \leq t_{K^*}^\uparrow \\ 1 & \text{otherwise} \end{cases} \quad (23)$$

Proof We will prove this using the KKT conditions, which are both necessary and sufficient for minimality for the Łukasiewicz t-norm since it is affine when the max constraint is not active. We drop the p -root in the norm since it is a strictly monotonically increasing function. The Lagrangian and corresponding derivative is

$$\begin{aligned} \ell &= \sum_{i=1}^n |\hat{t}_i - t_i|^p + \lambda (\max(\|\hat{\mathbf{t}}\|_1 + \|\mathbf{c}\|_1 - (m+n-1), 0) - \hat{t}_{T_L}) + \sum_{i=1}^n \gamma_i (\hat{t}_i - 1) \\ \frac{\partial \ell}{\partial \hat{t}_i} &= p(\hat{t}_i - t_i)^{p-1} + \lambda \frac{\partial}{\partial \hat{t}_i} \max(\|\hat{\mathbf{t}}\|_1 + \|\mathbf{c}\|_1 - (m+n-1), 0) + \gamma_i = 0. \end{aligned}$$

We note that we drop the absolute signs since T_L is strictly monotonically increasing function and $\hat{t}_{T_L} \geq T_L(\mathbf{t}, \mathbf{c})$. Assuming $\hat{t}_{T_L} > 0$, $T_L(\hat{\mathbf{t}}, \mathbf{c}) = \hat{t}_{T_L}$ can only be true if the first argument of max is chosen. Then for all $i, j \in \{1, \dots, n\}$, $p(\hat{t}_i - t_i)^{p-1} + \gamma_i = p(\hat{t}_j - t_j)^{p-1} + \gamma_j$. Define I as the set of K^* smallest t_i .

- *Primal feasibility:* For all $i \in I$, $\rho_{T_L}^*(\mathbf{t}, \hat{t}_{T_L})_i = \lambda_{K^*} \leq 1$ by definition. For all $i \in \{1, \dots, n\} \setminus I$, $\rho_{T_L}^*(\mathbf{t}, \hat{t}_{T_L})_i = 1 - t_i$. Furthermore,

$$\begin{aligned} T_L(\rho_{T_L}^*(\mathbf{t}, \hat{t}_{T_L}), \mathbf{c}) &= \max\left(\sum_{i=1}^{K^*} (t_i^\uparrow + \lambda_{K^*}) + \sum_{i=K^*+1}^n 1 + \|\mathbf{c}\|_1 - n - m + 1, 0\right) \\ &= \max\left(\sum_{i=1}^{K^*} t_i^\uparrow + K^* \lambda_{K^*} + n - K^* + \|\mathbf{c}\|_1 - n - m + 1, 0\right) \\ &= \max\left(\sum_{i=1}^{K^*} t_i^\uparrow + \hat{t}_{T_L} + m + K^* - 1 - \|\mathbf{c}\|_1 - \sum_{i=1}^{K^*} t_i^\uparrow \right. \\ &\quad \left. - K^* + \|\mathbf{c}\|_1 - m + 1, 0\right) = \hat{t}_{T_L} \end{aligned}$$

- *Complementary Slackness:* Clearly, for all $i \in I$, we require $\gamma_i = 0$. For all $i \in \{1, \dots, n\} \setminus I$, $\rho_{T_L}^*(\mathbf{t}, \hat{t}_{T_L})_i - 1 = 1 - 1 = 0$.
- *Dual feasibility:* For all $i \in I$, $\gamma_i = 0$. For $i \in \{1, \dots, n\} \setminus I$, consider some $j \in I$ and note that $p(\hat{t}_i - t_i)^{p-1} + \gamma_i = p(\hat{t}_j - t_j)^{p-1} + \gamma_j$. Filling in $\hat{\mathbf{t}}$, we find $\gamma_i = p\lambda_{K^*}^{p-1} - p(1 - t_i)^{p-1}$. This is nonnegative if $\lambda_{K^*} \geq 1 - t_i$. First, we show $\lambda_{K^*} \geq \lambda_{K^*+1}$. Write out their definitions, multiply by $K^*(K^* + 1)$ and remove common terms. Then,

$$\begin{aligned} \hat{t}_{T_L} + m - 1 - \|\mathbf{c}\|_1 - \sum_{i=1}^{K^*} t_i^\uparrow &\geq -K^* t_{K^*+1}^\uparrow \\ \hat{t}_{T_L} + m + K^* + 1 - \|\mathbf{c}\|_1 - \sum_{i=1}^{K^*+1} t_i^\uparrow &\geq (K^* + 1)(1 - t_{K^*+1}^\uparrow) \\ \lambda_{K^*+1} &\geq 1 - t_{K^*+1}^\uparrow. \end{aligned}$$

$\lambda_{K^*+1} \geq 1 - t_{K^*+1}^\uparrow$ is true by the construction in the proposition. Therefore,

$$\lambda_{K^*} \geq \lambda_{K^*+1} \geq 1 - t_{K^*+1}^\uparrow \geq 1 - t_i,$$

proving dual feasibility. □

A.2.2 Łukasiewicz t-conorm

Proposition 13. *The minimal refinement function of the Łukasiewicz t-conorm for $\hat{t}_{S_L} \in [S_L(\mathbf{t}, \mathbf{c}), \hat{t}_{S_L}]$ is*

$$\rho_{S_L}^*(\mathbf{t}, \hat{t}_{S_L})_i = t_i + \frac{\max(\hat{t}_{S_L} - \|\mathbf{t}\|_1 - \|\mathbf{c}\|_1, 0)}{n} \quad (24)$$

Proof We do not add multipliers for the constraints on \hat{t}_i , and show critical points adhere to these constraints. The Lagrangian is

$$\ell = \sum_{i=1}^n (\hat{t}_i - t_i)^p + \lambda(\min(\|\hat{\mathbf{t}}\|_1 + \|\mathbf{c}\|_1, 1) - \hat{t}_{S_L}) \quad (25)$$

Note that $\max_{S_L} = 1$. Taking the derivative to \hat{t}_i , we find

$$\frac{\partial \ell}{\partial \hat{t}_i} = p \cdot (\hat{t}_i - t_i)^{p-1} + \lambda \frac{\partial}{\partial \hat{t}_i} \min(\|\hat{\mathbf{t}}\|_1 + \|\mathbf{c}\|_1, 1) = 0$$

Assume $\hat{t}_{S_L} \neq S_L(\mathbf{t})$, this gives three cases for all $i \in \{1, \dots, n\}$:

1. If $\|\mathbf{t}\|_1 + \|\mathbf{c}\|_1 \geq 1$ and $\hat{t}_{S_L} = 1$, then since $\hat{t}_i \geq t_i$, $\frac{\partial}{\partial \hat{t}_i} \min(\|\hat{\mathbf{t}}\|_1 + \|\mathbf{c}\|_1, 1) = \frac{\partial}{\partial \hat{t}_i} 1 = 0$, and so $\hat{t}_i = t_i$.
2. If $\|\mathbf{t}\|_1 + \|\mathbf{c}\|_1 \geq 1$, then $\min_{S_L} = \max_{S_L} = 1$, and again $\hat{t}_i = t_i$.
3. Otherwise, it must be that $\|\hat{\mathbf{t}}\|_1 + \|\mathbf{c}\|_1 \leq 1$ and so $\frac{\partial}{\partial \hat{t}_i} \min(\|\hat{\mathbf{t}}\|_1 + \|\mathbf{c}\|_1, 1) = \frac{\partial}{\partial \hat{t}_i} \|\hat{\mathbf{t}}\|_1 = 1$, and therefore $p \cdot (\hat{t}_i - t_i)^{p-1} = -\lambda$. Since the equality holds for all $i \in \{1, \dots, n\}$, we find $p \cdot (\hat{t}_i - t_i)^{p-1} = p \cdot (\hat{t}_j - t_j)^{p-1}$ for all $i, j \in \{1, \dots, n\}$. As we are only interested in real nonnegative solutions, we find that $\hat{t}_i - t_i = \hat{t}_j - t_j = \delta$. Since $\|\hat{\mathbf{t}}\|_1 + \|\mathbf{c}\|_1 = \|\mathbf{t}\|_1 + \|\mathbf{c}\|_1 + n\delta = \hat{t}_{S_L}$, we find

$$\delta = \frac{\hat{t}_{S_L} - \|\mathbf{t}\|_1 - \|\mathbf{c}\|_1}{n}, \quad \hat{t}_i = t_i + \delta.$$

Note that $\hat{t}_i \geq t_i$, since by assumption $\hat{t}_{S_L} \geq S_L(\mathbf{t}, \mathbf{c})$, and $\hat{t}_i \leq 1$ since by $\hat{t}_{S_L} \leq \max_{S_L} \leq 1$, $\delta = \frac{\hat{t}_{S_L} - \|\mathbf{t}\|_1 - \|\mathbf{c}\|_1}{n} \leq \frac{1 - \|\mathbf{t}\|_1 - \|\mathbf{c}\|_1}{n} \leq \frac{1 - t_i}{n} \leq 1 - t_i$, that is, the constraints of Equation 7 are satisfied. \square

B Dual Problem

This section introduces a dual problem to Equation 7. This is used extensively in several proofs.

B.1 Strict cone monotonicity

Definition 10. A set $K \subset [0, 1]^n$ is a (*convex*) *cone* if for every $s > 0$ and $\mathbf{t} \in K$ such that $s\mathbf{t} \in [0, 1]^n$, also $s\mathbf{t} \in K$.

A fuzzy evaluation operator f_φ is *strictly cone-increasing* at $\mathbf{t} \in [0, 1]^n$ if there is a nonempty cone $K(\mathbf{t})$ such that $\mathbf{t}' - \mathbf{t} \in K$ implies $f_\varphi(\mathbf{t}) < f_\varphi(\mathbf{t}')$.

Strict cone-monotonicity is a weak notion of monotonicity in the sense that all t-norms that are strictly increasing in each argument are strictly cone-increasing, but the reverse need not be true.

Proposition 14. *If f_φ is non-decreasing and strictly cone-increasing at $\mathbf{t} \in [0, 1]^n$, there exist a nonempty cone $K'(\mathbf{t}) \subseteq K(\mathbf{t})$ such that $\mathbf{t}' - \mathbf{t} \in K'(\mathbf{t})$ implies $\mathbf{t}'_i \geq t_i$ for all $i \in \{0, \dots, n\}$.*

Proof Assume otherwise. Consider some \mathbf{t}' such that $s(\mathbf{t}' - \mathbf{t}) \in K(\mathbf{t})$ for $s > 0$. By assumption, there is some $i \in \{0, \dots, n\}$ such that $\mathbf{t}'_i < t_i$. Consider $\hat{\mathbf{t}}$ equal to \mathbf{t}' except that $\hat{t}_i = t_i$ for such i . Since f_φ is non-decreasing in each argument, $f_\varphi(\hat{\mathbf{t}}) \geq f_\varphi(\mathbf{t}') > f_\varphi(\mathbf{t})$, then clearly $s(\hat{\mathbf{t}} - \mathbf{t})$ for $s > 0$ forms the cone $K'(\mathbf{t})$. \square

B.2 Dual problem

Next, we will investigate a dual problem for the problem in Equation 7 that will allow us to prove multiple useful theorems:

$$\begin{aligned} \text{For all } \mathbf{t} \in [0, 1]^n, u \in [0, \infty) : \\ \max_{\hat{\mathbf{t}}} f_\varphi(\hat{\mathbf{t}}) \\ \text{such that } \|\hat{\mathbf{t}} - \mathbf{t}\| = u, \\ 0 \leq \hat{t}_i \leq 1. \end{aligned} \tag{26}$$

That is, instead of finding the $\hat{\mathbf{t}}$ closest to \mathbf{t} with refinement value \hat{t}_φ , we find the largest refined value attainable with a fixed budget u . We need to be precise when solutions of this dual problem coincide with the problem in Equation 7. We consider strict cone-monotonicity [6, 31], which is a weak notion of strict monotonicity for higher dimensions. This intuitively means that there is always some direction we can move in to increase the value of the t-norm. Since t-norms are already non-decreasing in each argument, this implies there is no point where the t-norm is “flat” in all directions. The precise definition is given in Definition 10.

Theorem 3. *A solution \mathbf{t}^* for some f_φ , \mathbf{t} and $u \geq 0$ of Equation 26 is also a solution to Equation 7 for \mathbf{t} and $\hat{t}_\varphi = f_\varphi(\mathbf{t}^*) \geq f_\varphi(\mathbf{t})$ if f_φ is non-decreasing in all arguments and strictly cone-increasing at each $\mathbf{t}' \in [0, 1]^n$ such that $f_\varphi(\mathbf{t}') = \hat{t}_\varphi$, and if $\|\cdot\|$ is strictly increasing in all arguments.*

Proof Assume otherwise, and suppose a solution $\hat{\mathbf{t}}$ for Equation 7 exists such that $f_\varphi(\hat{\mathbf{t}}) = \hat{t}_\varphi$ while $\|\hat{\mathbf{t}} - \mathbf{t}\| < \|\mathbf{t}^* - \mathbf{t}\| = u$. Since f_φ is non-decreasing in all arguments and $\hat{t}_\varphi \geq f_\varphi(\mathbf{t})$, $\hat{\mathbf{t}} - \mathbf{t}$ and $\mathbf{t}^* - \mathbf{t}$ are nonnegative. By Proposition 14 there is some cone $K(\hat{\mathbf{t}})$ that contains a line segment $\epsilon(s) = s(\mathbf{t}' - \hat{\mathbf{t}})$ such that for all $s > 0$, $f_\varphi(\hat{\mathbf{t}}) < f_\varphi(\hat{\mathbf{t}} + \epsilon(s))$ and for all $i \in \{0, \dots, n\}$, $0 \leq \epsilon(s)_i$. Therefore, necessarily there is some i such that $0 < \epsilon(s)_i$. Since $\|\cdot\|$ is strictly increasing on nonnegative

vectors and continuous (since it is a norm), necessarily there is some $s > 0$ such that $\|\hat{\mathbf{t}} + \epsilon(s)\| = u$. However, this is in contradiction with the premise that \mathbf{t}^* is a solution of Equation 26, as $f_\varphi(\hat{\mathbf{t}} + \epsilon(s)) > f_\varphi(\mathbf{t}^*)$. \square

Since $f_\varphi \in [0, 1]^n \rightarrow [0, 1]$, f_φ cannot satisfy the conditions of Theorem 3 when $\hat{t}_\varphi = 1$. For all $\hat{t}_\varphi \in [0, 1)$ however, both the Gödel and product t-norms and t-conorms are strictly cone-increasing. The Łukasiewicz t-norm satisfies the conditions for $\hat{t}_\varphi \in (0, 1)$, since it has flat regions for $\hat{t}_\varphi = 0$. The same reasoning can be made for the nilpotent minimum and drastic t-norms, see [32]. Furthermore, all t-norms with an additive generator are strictly cone-increasing on $\hat{t}_\varphi \in (0, 1)$, as are all strict t-norms.

C Schur-concave t-norms (Proofs)

C.1 Minimal refinement function for t-norms

Theorem 4. *Let T be a Schur-concave t-norm that is strictly cone-increasing at \hat{t}_T and let $\|\cdot\|$ be a strict norm. Then there is a minimal refined vector \mathbf{t}^* for \mathbf{t} and \hat{t}_T such that whenever $t_i > t_j$, then $t_i^* - t_i \leq t_j^* - t_j$.*

Proof Assume there is a minimal refined vector $\hat{\mathbf{t}} \neq \mathbf{t}^*$ which has some $\hat{t}_i - t_i > \hat{t}_j - t_j$ while $t_i > t_j$. Consider $\hat{\mathbf{t}}'$ equal to $\hat{\mathbf{t}}$ except that $\hat{t}'_i = \hat{t}_j - t_j + t_i$ and $\hat{t}'_j = \hat{t}_i - t_i + t_j$ such that by symmetry $\|\hat{\mathbf{t}} - \mathbf{t}\| = \|\hat{\mathbf{t}}' - \mathbf{t}\|$. Define $\hat{t}'_{\max} = \max(\hat{t}'_i, \hat{t}'_j)$ and $\hat{t}'_{\min} = \min(\hat{t}'_i, \hat{t}'_j)$. Clearly, $\hat{t}_i > \hat{t}'_{\max} \geq \hat{t}'_{\min} > \hat{t}_j$. We will show $\hat{\mathbf{t}}$ majorizes $\hat{\mathbf{t}}'$ by checking the condition of Definition 8 for any $k \in \{1, \dots, n\}$.

1. If $\hat{t}_k > \hat{t}_i$, then all elements are equal and $\sum_{l=1}^k \hat{t}_l^\downarrow = \sum_{l=1}^k \hat{t}'_l^\downarrow$.
2. If $\hat{t}_i \geq \hat{t}_k > \hat{t}'_{\max}$, then $\sum_{l=1}^k \hat{t}_l^\downarrow = \sum_{l=1}^{k-1} \hat{t}'_l^\downarrow + \hat{t}_i \geq \sum_{l=1}^k \hat{t}'_l^\downarrow$.
3. If $\hat{t}'_{\max} \geq \hat{t}_k > \hat{t}'_{\min}$, then $\sum_{l=1}^k \hat{t}_l^\downarrow > \sum_{l=1}^k \hat{t}'_l^\downarrow$, since by removing common terms we get $\hat{t}_i > \hat{t}'_{\max}$.
4. If $\hat{t}'_{\min} \geq \hat{t}_k > \hat{t}_j$, then removing all common terms in the sums, we are left with $\hat{t}_i + \hat{t}_k > \hat{t}'_{\min} + \hat{t}'_{\max}$. Note $\hat{t}'_{\min} + \hat{t}'_{\max} = \hat{t}_j + t_i - t_j + \hat{t}_i + t_j - t_i = \hat{t}_i + \hat{t}_j$. Subtracting \hat{t}_i from both sides, we are left with $\hat{t}_k > \hat{t}_j$, which is true by assumption.
5. If $\hat{t}'_{\min} \geq \hat{t}_k$, then removing common terms, we are left with $\hat{t}'_{\max} + \hat{t}'_{\min} = \hat{t}_i + \hat{t}_j$.

Therefore, $\hat{\mathbf{t}}$ majorizes $\hat{\mathbf{t}}'$, and so by Schur concavity, $T(\hat{\mathbf{t}}, \mathbf{c}) \leq T(\hat{\mathbf{t}}', \mathbf{c})$, noting that the additional truth vector \mathbf{c} will not influence the majorization result since it is applied at both sides. By Theorem 3, either 1) $T(\hat{\mathbf{t}}, \mathbf{c}) < T(\hat{\mathbf{t}}', \mathbf{c})$, so $\hat{\mathbf{t}}$ could not have been minimal, leading to a contradiction, or 2) $T(\hat{\mathbf{t}}, \mathbf{c}) = T(\hat{\mathbf{t}}', \mathbf{c})$ and both $\hat{\mathbf{t}}$ and $\hat{\mathbf{t}}'$ are minimal. \square

C.2 Closed-form refinement function using additive generators

Proposition 15. *Let T be a Schur-concave t -norm with additive generator g and let $0 < \hat{t}_T \in [T(\mathbf{t}, \mathbf{c}), \max_T]$. Let $K \in \{0, \dots, n-1\}$ denote the number of truth values such that $t^*_i = t_i$ in Equation 28. Then using*

$$\lambda_K = g^{-1} \left(\frac{1}{n-K} \left(g(\hat{t}_T) - \sum_{i=1}^K g(t_i^\downarrow) - \sum_{i=1}^m g(C_i) \right) \right) \quad (27)$$

in Equation 28 gives $T(\mathbf{t}^*, \mathbf{c}) = \hat{t}_T$ if $\mathbf{t}^* \in [0, 1]^n$.

Proof Using Equations 15 and 28, we find that

$$T(\mathbf{t}^*, \mathbf{c}) = g^{-1} \left(\min \left(g(0^+), \sum_{i=1}^K g(t_i^\downarrow) + \sum_{i=K+1}^n g(\lambda_K) + \sum_{i=1}^m g(C_i) \right) \right) = \hat{t}_T$$

Since $\hat{t}_T > 0$, we can remove the min, since $\hat{t}_T > 0$ will require that $\sum_{i=1}^K g(t_i^\downarrow) + (n-K)g(\lambda_K) + \sum_{i=1}^m g(C_i) > g(0^+)$. We apply g to both sides of the equation, which is allowed since g is a bijection. Thus

$$\begin{aligned} g(\hat{t}_T) &= \sum_{i=1}^K g(t_i^\downarrow) + (n-K)g(\lambda_K) + \sum_{i=1}^m g(C_i) \\ g(\lambda_K) &= \frac{1}{n-K} \left(g(\hat{t}_T) - \sum_{i=1}^K g(t_i^\downarrow) - \sum_{i=1}^m g(C_i) \right) \\ \lambda_K &= g^{-1} \left(\frac{1}{n-K} \left(g(\hat{t}_T) - \sum_{i=1}^K g(t_i^\downarrow) - \sum_{i=1}^m g(C_i) \right) \right), \end{aligned}$$

where in the last step we apply g^{-1} . \square

In a similar manner we can find the λ for the t -conorm. Let $j = \arg \max_{i=1}^n t_i$.

$$\begin{aligned} S(\mathbf{t}^*) &= 1 - g^{-1}(\min(g(0^+), \sum_{i=1}^n g(1-t^*_i) + \sum_{i=1}^m g(1-C_i))) = \hat{t}_S \\ \min(g(0^+), g(1-\lambda) + \sum_{i \neq j} g(1-t_i) + \sum_{i=1}^m g(1-C_i)) &= g(1-\hat{t}_S) \end{aligned}$$

If $\hat{t}_S < 1$, or if $g(0)$ is well defined, then we can ignore the min:

$$\begin{aligned} g(1-\lambda) &= g(1-\hat{t}_S) - \sum_{i \neq j} g(1-t_i) - \sum_{i=1}^m g(1-C_i) \\ \lambda &= 1 - g^{-1} \left(g(1-\hat{t}_S) - \sum_{i \neq j} g(1-t_i) - \sum_{i=1}^m g(1-C_i) \right) \end{aligned}$$

C.3 L1 minimal refinement function for t-norms

Proposition 16. *Let $\mathbf{t} \in [0, 1]^n$ and let T be a Schur-concave t-norm that is strictly cone-increasing at $\hat{t}_T \in [T(\mathbf{t}, \mathbf{c}), \max_T]$. Then there is a value $\lambda \in [0, 1]$ such that the vector \mathbf{t}^* ,*

$$t^*_i = \begin{cases} \lambda, & \text{if } t_i < \lambda, \\ t_i, & \text{otherwise,} \end{cases} \quad (28)$$

is a minimal refined vector for T and the L1 norm at \mathbf{t} and \hat{t}_T .

Proof Assume otherwise. Then, using Theorem 3, there must be a refined vector $\hat{\mathbf{t}}$ such that $\|\hat{\mathbf{t}} - \mathbf{t}\|_1 = \|\mathbf{t}^* - \mathbf{t}\|_1$ but $T(\hat{\mathbf{t}}, \mathbf{c}) > T(\mathbf{t}^*, \mathbf{c})$. Since $\hat{t}_T \in [T(\mathbf{t}, \mathbf{c}), \max_T]$, we can assume $\hat{t}_i \geq t_i$. We define $\pi^*(i)$ as the permutation in descending order of \mathbf{t}^* . Furthermore, let k be the smallest j such that $t_j^\downarrow < \lambda$.

Since $\|\hat{\mathbf{t}}\|_1 = \|\mathbf{t}^*\|_1$, by assumption of equal L1 norms of $\hat{\mathbf{t}}$ and \mathbf{t}^* , we will prove for all $i \in \{1, \dots, n\}$ that $\hat{\mathbf{t}}$ majorizes \mathbf{t}^* .

- If $i < k$, then $\sum_{j=1}^i \hat{t}_j^\downarrow \geq \sum_{j=1}^i \hat{t}_{\pi^*(j)}^\downarrow \geq \sum_{j=1}^i t_{\pi^*(j)}^\downarrow = \sum_{j=1}^i t_j^{*\downarrow}$. The first inequality follows from the fact that there is no ordering of $\hat{\mathbf{t}}$ that will have a higher sum than in descending order.
- If $i \geq k$, then clearly $t_i^{*\downarrow} = \lambda$. Furthermore, $\sum_{j=1}^i t_j^{*\downarrow} = \sum_{j=1}^k t_j^\downarrow + (i - k)\lambda$. We will distinguish two cases:
 1. $\hat{t}_i^\downarrow \geq \lambda$. Then for all $j \in \{k, \dots, i\}$, $\hat{t}_j^\downarrow \geq \lambda$. Furthermore, from the previous result, $\sum_{j=1}^{k-1} \hat{t}_j^\downarrow \geq \sum_{j=1}^{k-1} t_j^{*\downarrow}$ and so clearly $\sum_{j=1}^i \hat{t}_j^\downarrow \geq \sum_{j=1}^i t_j^{*\downarrow}$.
 2. $\hat{t}_i^\downarrow < \lambda$. Then for all $j > i$, $\hat{t}_j^\downarrow \leq \hat{t}_i^\downarrow < \lambda$, and so $\sum_{j=i+1}^n \hat{t}_j^\downarrow \leq \sum_{j=i+1}^n \hat{t}_i^\downarrow = (n - i)\hat{t}_i^\downarrow < (n - i)\lambda$. Using this, we note that

$$\|\mathbf{t}^*\|_1 = \sum_{j=1}^k t_j^\downarrow + (n - k)\lambda = \|\hat{\mathbf{t}}\|_1 = \sum_{j=1}^i \hat{t}_j^\downarrow + \sum_{j=i+1}^n \hat{t}_j^\downarrow < \sum_{j=1}^i \hat{t}_j^\downarrow + (n - i)\lambda.$$

Then, subtracting $(n - i)\lambda$ from the inequality, we find

$$\sum_{j=1}^i \hat{t}_j^\downarrow > \sum_{j=1}^k t_j^\downarrow + (n - k)\lambda - (n - i)\lambda = \sum_{j=1}^k t_j^\downarrow + (i - k)\lambda = \sum_{j=1}^i t_j^{*\downarrow}$$

And so, $\hat{\mathbf{t}}$ majorizes \mathbf{t}^* , and by Schur concavity of T , $T(\hat{\mathbf{t}}, \mathbf{c}) \leq T(\mathbf{t}^*, \mathbf{c})$ leading to a contradiction. \square

C.4 L1 minimal refinement function for t-conorms

Proposition 17. *Let $\mathbf{t} \in [0, 1]^n$ and let S be a Schur-convex t-conorm that is strictly cone-increasing at $\hat{t}_S \in [S(\mathbf{t}, \mathbf{c}), 1]$. Then there is a value $\lambda \in [0, 1]$*

such that the vector \mathbf{t}^* ,

$$t^*_i = \begin{cases} \lambda & \text{if } i = \arg \max_{i \in D} t_i, \\ t_i, & \text{otherwise,} \end{cases} \quad (29)$$

is a minimal refined vector for S and the $L1$ norm at \mathbf{t} and \hat{t}_S .

Proposition 18. *Let $\mathbf{t} \in [0, 1]^n$ and let S be a Schur-convex t -conorm that is strictly cone-increasing at $\hat{t}_S \in [S(\mathbf{t}, \mathbf{c}), 1]$. Then there is a value $\lambda \in [0, 1]$ such that the vector \mathbf{t}^* with $i \in D$,*

$$t^*_i = \begin{cases} \lambda & \text{if } i = \arg \max_{i \in D} t_i, \\ t_i, & \text{otherwise,} \end{cases} \quad (30)$$

is a minimal refined vector for S and the $L1$ norm at \mathbf{t} and \hat{t}_S .

Proof Assume otherwise. Then, using Theorem 3, there must be a refined vector $\hat{\mathbf{t}} \neq \mathbf{t}^*$ such that $\|\hat{\mathbf{t}} - \mathbf{t}\|_1 = \|\mathbf{t}^* - \mathbf{t}\|_1 = \lambda - t_1^\downarrow$ but $S(\hat{\mathbf{t}}, \mathbf{c}) > S(\mathbf{t}^*, \mathbf{c})$. Let $\pi(i)$ be the permutation in descending order of $\hat{\mathbf{t}}$.

Consider any $k \in \{1, \dots, n\}$. Then $\sum_{i=1}^k t^{*\downarrow}_i = \sum_{i=1}^k t_i^\downarrow + (\lambda - t_1^\downarrow)$, while $\sum_{i=1}^k \hat{t}_j^\downarrow = \sum_{i=1}^k t_{\pi(i)} + \sum_{i=1}^k (\hat{t}_i - t_{\pi(i)})$. There is no permutation with higher sum than in descending order, so $\sum_{i=1}^k t_{\pi(i)} \leq \sum_{i=1}^k t_i^\downarrow$. Furthermore, since $\|\hat{\mathbf{t}} - \mathbf{t}\|_1 = \lambda - t_1^\downarrow$, $\sum_{i=1}^k (\hat{t}_i - t_{\pi(i)}) \leq \lambda - t_1^\downarrow$. Therefore, $\sum_{i=1}^k \hat{t}_i^\downarrow \leq \sum_{i=1}^k t^{*\downarrow}_i$, that is, \mathbf{t}^* majorizes $\hat{\mathbf{t}}$, and by Schur convexity of S , $S(\mathbf{t}^*, \mathbf{c}) \geq S(\hat{\mathbf{t}}, \mathbf{c})$. \square

C.5 L1 minimal refinement function for residuums

Proposition 19. *Let $t_1, t_2 \in [0, 1]$ and let T be a strict Schur-concave t -norm with additive generator g . Consider its residuum $R(t_1, t_2) = \sup\{z | T(t_1, z) \leq t_2\}$ that is strictly cone-increasing at $0 < \hat{t}_R \in [R(t_1, t_2), \max_R]$. Then there is a value $\lambda \in [0, 1]$ such that $\mathbf{t}^* = [t_1, \lambda]^\top$ is a minimal refined vector for R and the $L1$ norm at \mathbf{t} and t .*

Proof We will assume $t_1 > t_2$, as otherwise $R(t_1, t_2) = 1$ for any residuum, which necessarily means $\hat{t}_R = 1$ and so $\mathbf{t}^* = \mathbf{t}$. Assume \mathbf{t}^* is not minimal. Since R is strictly cone increasing at \hat{t}_R , by Theorem 3⁵ there must be some $\hat{\mathbf{t}}$ such that $\|\hat{\mathbf{t}} - \mathbf{t}\| = \|\mathbf{t}^* - \mathbf{t}\| = \lambda - t_2$ but $R(\hat{t}_1, \hat{t}_2) > R(t^*_1, t^*_2)$. Since R is non-decreasing in the first argument and non-increasing in the second, we consider $\hat{\mathbf{t}} = [t_1 - \epsilon, \lambda - \epsilon]^\top$ for $\epsilon > 0$.

The residuum constructed from continuous t -norms with an additive generator can be computed as $R(t_1, t_2) = g^{-1}(\max(g(t_2) - g(t_1), 0))$. Since we assumed $R(t^*_1, t^*_2) < R(\hat{t}_1, \hat{t}_2)$, applying g to both sides,

$$\max(g(\lambda) - g(t_1), 0) > \max(g(\lambda - \epsilon) - g(t_1 - \epsilon), 0)$$

⁵This theorem has to be adjusted for the fact that fuzzy implications are non-increasing in the first argument. It can be applied by considering $1 - t_1$.

$$\begin{aligned} g^{-1}(g(\lambda) + g(t_1 - \epsilon)) &< g^{-1}(g(\lambda - \epsilon) + g(t_1)) \\ T(\lambda, t_1 - \epsilon) &< T(\lambda - \epsilon, t_1) \end{aligned}$$

where in the second step we assume $\lambda \leq t_1$, that is, we are not setting new consequent larger than the antecedent, as otherwise we could find a smaller refined vector by setting it to exactly t_1 . In the last step we use that T is strict, as then $T(t_1, t_2) = g^{-1}(g(t_1) + g(t_2))$. We now use the majorization as $\lambda + t_1 - \epsilon = \lambda - \epsilon + t_1$.

Since $\lambda \leq t_1$, surely $t_1 > \lambda - \epsilon$. Then there are two cases:

1. $\lambda \geq t_1 - \epsilon$. Then $t_1 \geq \lambda$ as assumed.
2. $t_1 - \epsilon \geq \lambda$. Then clearly $t_1 \geq t_1 - \epsilon$ as $\epsilon > 0$.

Therefore $[\lambda - \epsilon, t_1]^\top$ majorizes $[\lambda, t_1 - \epsilon]^\top$, and by Schur concavity $T(\lambda, t_1 - \epsilon) \geq T(\lambda - \epsilon, t_1)$ which is a contradiction. \square

D Product t-norm with L2 norm

In this appendix, we consider the refinement functions for the product t-norm under the L2-norm. We find that there is no simple closed-form parameterization in terms of \hat{t}_φ , but we can find approximations in linear time. These are satisfactory to reliably find the minimal refinement function.

In the following, we will ignore constants and consider formulas $\bigwedge_{i=1}^n P_i$, and consider the problem in Equation 7. We consider the logarithm of the product as its optimum coincides.

$$\begin{aligned} \text{For all } \mathbf{t} \in [0, 1]^n, \hat{t}_{T_P} \in [T_P(\mathbf{t}), 1] \\ \min_{\hat{\mathbf{t}}} \sum_{i=1}^n (\hat{t}_i - t_i)^2 \\ \text{such that } \sum_{i=1}^n \log \hat{t}_i = \log \hat{t}_{T_P} \\ \hat{t}_i - 1 \leq 0 \end{aligned} \tag{31}$$

With Lagrangian $L = \sum_i (\hat{t}_i - t_i)^2 + \lambda (\sum_i \log \hat{t}_i - \log \hat{t}_{T_P}) - \gamma_i (\hat{t}_i - 1)$, and so

$$\begin{aligned} \frac{\partial L}{\partial \hat{t}_i} &= 2(\hat{t}_i - t_i) - \gamma_i + \frac{\lambda}{\hat{t}_i} = 0 \\ \lambda &= (\gamma + 2t_i - 2\hat{t}_i)\hat{t}_i \end{aligned}$$

Since this holds for all i , we find that for all i, j , $(\gamma + 2t_i - 2\hat{t}_i)\hat{t}_i = (\gamma + 2t_j - 2\hat{t}_j)\hat{t}_j = \lambda$. We partition $\{1, \dots, n\}$ into sets I and M , where I contains all i such that $\hat{t}_i < 1$, and M those where $\hat{t}_i = 1$. For $i \in I$, by noting that using the complementary slackness condition $\gamma_i = 0$, this induces a quadratic equation in \hat{t}_i with solutions

$$\hat{t}_i = \frac{1}{2}(t_i \pm \sqrt{t_i^2 - 2\lambda}). \tag{32}$$

Since we assume $\hat{t}_i \geq t_i$, we have to take the solution that adds the root of the determinant, that is, $\hat{t}_i = \frac{1}{2}(\sqrt{t_i^2 - 2\lambda} + t_i)$. Furthermore, since we constrain for $i \in I$ that $\hat{t}_i < 1$, we find that

$$\begin{aligned} 1 &> \frac{1}{2}(t_i + \sqrt{t_i^2 - 2\lambda}) \\ 2 - t_i &> \sqrt{t_i^2 - 2\lambda} \\ \lambda &> 2t_i - 2. \end{aligned}$$

Therefore, given some chosen value of c , we require for all $i \in I$ that $\lambda > 2t_i - 2$, and so,

$$\min_{i \in I} 2t_i - 2 > \lambda$$

Unfortunately, finding the exact value of λ such that $T_P(\hat{\mathbf{t}}) = \hat{t}_{T_P}$ is a challenge. Filling in \hat{t}_i , we find

$$T_P(\hat{\mathbf{t}}) = \prod_{i=1}^n (\hat{t}_i) = \prod_{i \in I} \frac{1}{2}(t_i + \sqrt{t_i^2 - 2\lambda}) = \hat{t}_{T_P}. \quad (33)$$

This is a $2n$ -th degree polynomial in λ , and we were not able to find an obvious, general closed form solution to it. Mathematica [19] finds a complicated closed form formula for $n = 2$, but cannot find closed form formulas for $n > 2$.

We also still need to figure out how to partition $i = \{1, \dots, n\}$ into I and M . Since \hat{t}_i as computed by Equation 32 is a strictly decreasing function in λ for all $i \in I$, we have the following unproven proposition. It supports the result given in Theorem 4.

Proposition 20. *For all $\lambda \in [\min_{i=1}^n 2t_i - 2, 0]$, the function*

$$\rho_{T_P}^*(\mathbf{t}, \lambda)_i = \begin{cases} \frac{1}{2}(t_i + \sqrt{t_i^2 - 2\lambda}) & \text{if } 2t_i - 2 > \lambda, \\ 1 - t_i & \text{otherwise.} \end{cases} \quad (34)$$

has the following properties:

1. $\rho_{T_P}^*(\mathbf{t}, \lambda)$ is a minimal refinement vector for the product t -norm, the $L2$ norm and $\hat{t}_{T_P} = T_P(\rho_{T_P}^*(\mathbf{t}, \lambda))$;
2. $\hat{t}_{T_P} = T_P(\rho_{T_P}^*(\mathbf{t}, \lambda))$ is a strictly decreasing function in c on $(\min_{i=1}^n 2t_i - 2, 0]$, and so there is a bijection between λ and $t \in [T_P(\mathbf{t}), 1]$ on this interval.

The second property is easy to see by noting the derivative of $\rho_{T_P}^*(\mathbf{t}, \lambda)$ is negative on $\lambda \in (\min_{i=1}^n 2t_i - 2]$, but for the first we do not have a direct proof as of yet and leave this for future work.

Although $\rho_{T_P}^*(\mathbf{t}, \lambda)$ is not parameterized in terms of \hat{t}_{T_P} , it can still be used in practical scenarios where λ can be seen as the negative ‘‘confidence’’ in the clause. A practical implementation could learn a weight for the clause between

0 and 1, and then transform it to the domain of λ by dividing by $\min_{i=1}^n 2t_i - 2$. Alternatively, $\|T_P(\mathbf{t} + \rho_{T_P}^*(\mathbf{t}, \lambda)) - \hat{t}_{T_P}\|_2$ can be minimized with respect to λ using mathematical optimization methods like gradient descent or Newton's method to find answers in terms of \hat{t}_{T_P} .

E Additional experiments

In this Appendix we present additional experiments when \hat{t}_φ is not 1.

E.1 Results - Refined value 0.3

The figures in this section present the results when the refined value $\hat{t}_\varphi = 0.3$.

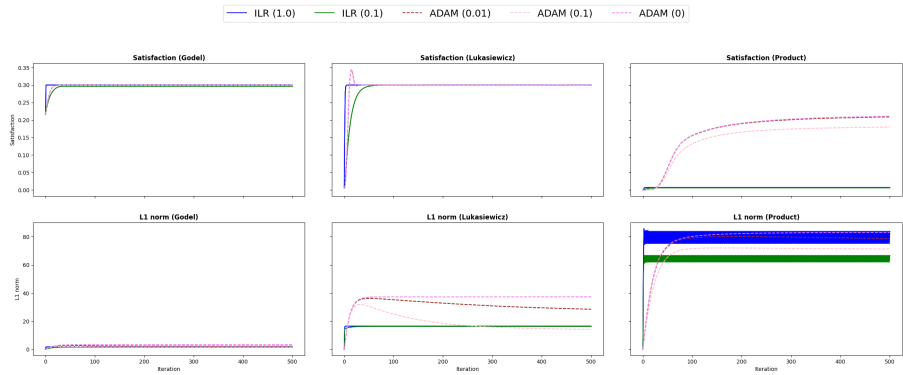


Fig. 10 Comparison of ILR with ADAM on uf20-91 of SATLIB. Refined value 0.3. The x axis corresponds to the number of iterations, while the y axis is the value of \hat{t}_φ in the first row of the grid, and the L1 norm in the second row.

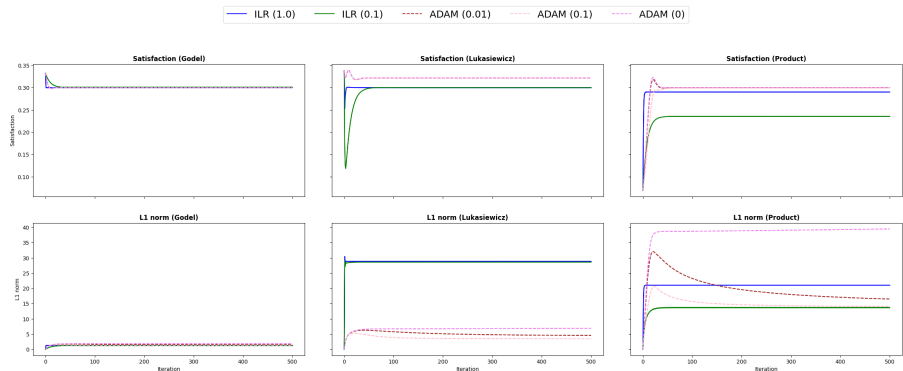


Fig. 11 Comparison of ILR with ADAM on the uf20-91 with 20 clauses. Refined value 0.3.

E.2 Results - Refined value 0.5

The figures in this section present the results when the refined value $\hat{t}_\varphi = 0.5$. We note that the satisfaction for ADAM in Łukasiewicz converges above 0.5 in Figure 13. This means the final truth value is too high, and it has not found a proper solution here.

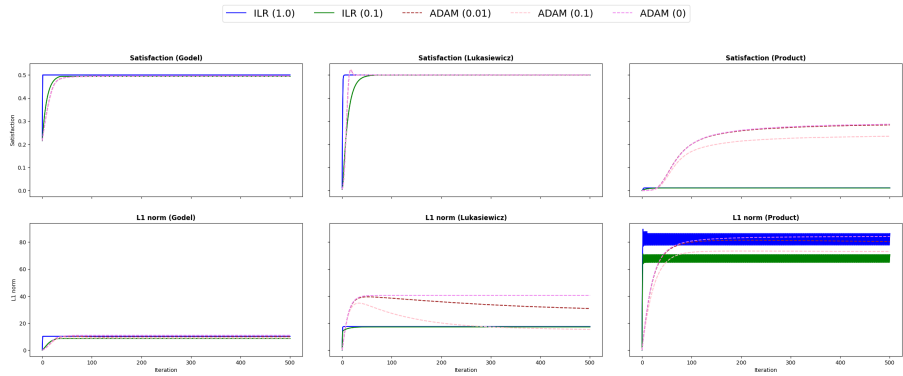


Fig. 12 Comparison of ILR with ADAM on the uf20-91 of SATLIB. Refined value 0.5.

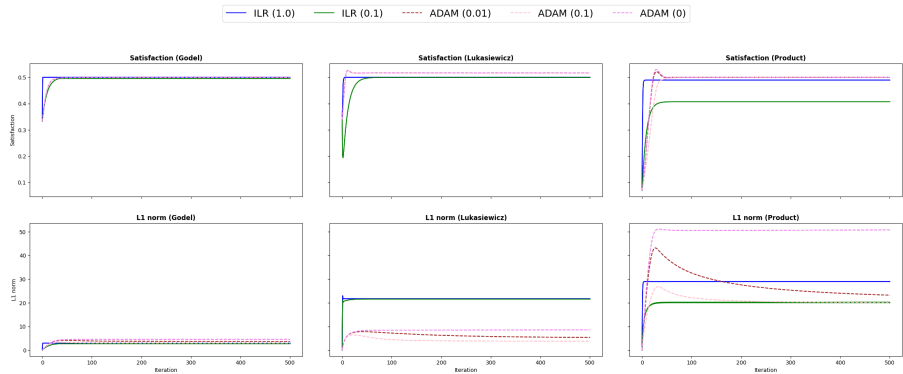


Fig. 13 Comparison of ILR with ADAM on the uf20-91 with 20 clauses. Refined value 0.5.